Abstract and Applied Analysis

WILEY

RESEARCH ARTICLE OPEN ACCESS

Mathematical Analysis of a Reaction-Diffusion Pneumococcal Pneumonia Epidemic Model

Amos Ainembabazi | Michael Byamukama | Martin Karuhanga

Department of Mathematics, Mbarara University of Science and Technology, P.O. Box 1410, Mbarara, Uganda

Correspondence: Martin Karuhanga (mkaruhanga@must.ac.ug)

Received: 17 July 2026 | **Revised:** 7 September 2026 | **Accepted:** 14 October 2026

Academic Editor: Patricia J. Y. Wong

Keywords: effective reproduction number | pneumococcal pneumonia | reaction-diffusion | treatment | vaccination

ABSTRACT

Pneumococcal pneumonia, caused by *Streptococcus pneumoniae*, remains a significant health threat, particularly for children, the elderly, and immunocompromised individuals. This study presents a reaction-diffusion model using partial differential equations. The model ensures the positivity and boundedness of all solutions. The model also exhibits both disease-free and endemic equilibrium solutions. The effective reproduction number, $\mathscr{R}_e$ is derived and conditions for the asymptotic stability of both the disease-free and endemic equilibrium are established. Sensitivity analysis highlights the parameters which are critical in the disease transmission. Numerical simulations confirm the global asymptotic stability of the equilibrium points. The findings further indicate that a combined strategy of vaccination and treatment is more effective than treatment alone in controlling infections and curbing disease transmission, whereas elevated vaccine failure rates are observed to weaken the overall control efforts against pneumococcal pneumonia.

1 | Introduction

Pneumonia is a form of acute respiratory infection that affects the lungs [1]. The lungs are composed of small air sacs known as alveoli, which are filled with air during normal breathing. In individuals with pneumonia, these alveoli become inflamed and fill with pus or fluid causing painful breathing and reducing oxygen intake [2]. Pneumonia is caused by various pathogens, including bacteria, viruses, and fungi. Fungal infections can result into Cryptococcus, *Pneumocystis jirovecii*, and Coccidioides forms of pneumonia [3]. Viral infections, on the other hand, lead to respiratory syncytial virus (RSV) form of pneumonia, whereas bacterial infections caused by *Streptococcus pneumoniae* can lead to pneumococcal pneumonia [3]. *Streptococcus pneumoniae* was first identified by Louis Pasteur and George M. Sternberg in the late 19th century and was later recognized as the main cause of pneumonia [4].

Pneumonia is broadly categorized based on how the infection is acquired. These categories include community-acquired pneumonia (CAP) and nosocomial pneumonia, which encompasses hospital-acquired pneumonia (HAP), ventilator-associated pneumonia (VAP), and healthcare-associated pneumonia (HCAP) [5]. According to WHO, CAP is the most prevalent form and poses a major global health challenge, accounting for ~3 million deaths annually world wide [6]. Bacterial pathogens are the predominant cause of CAP, with *Streptococcus pneumoniae* being the most frequent culprit.

Pneumococcal pneumonia is one of the leading causes of morbidity and mortality globally, particularly in children, elderly, and individuals with weakened immune systems [7]. It is highly contagious, spreading through inhalation of droplets from an infected person's cough or sneeze, as well as via microaspiration of bacteria from the throat, especially among children who often

This is an open access article under the terms of the Creative Commons Attribution License, which permits use, distribution and reproduction in any medium, provided the original work is properly cited.

Copyright © 2026 Amos Ainembabazi et al. *Abstract and Applied Analysis* published by John Wiley & Sons Ltd.

carry the bacteria without showing symptoms [8]. The incubation period of pneumococcal pneumonia typically ranges from 1 to 3 days, and after this period, the infected individual starts showing symptoms like high fever, headache, coughing, hypothermia, lethargy, and other common flu symptoms [9]. Carriers often harbor the pathogen without showing symptoms, allowing them to move freely and interact with others, thereby facilitating silent transmission across the population, and if left uncontrolled, they can sustain the circulation of the pathogen and contribute to the persistence of the disease at an endemic level [10].

Worldwide, it is estimated that around 14.5 million cases of severe pneumococcal disease affect children under the age of five annually, leading to ~500,000 deaths [11]. While it impacts children and families across the globe, it is most common in South Asia and sub-Saharan Africa [2]. Several factors increase the risk of contracting pneumococcal pneumonia. These include drug abuse, insufficient breastfeeding, chronic heart diseases, chronic obstructive pulmonary disease (COPD), malnutrition, overcrowded living environments, indoor air pollution, and prior viral infections [12, 13].

The WHO and UNICEF jointly launched the Global Action Plan for the Prevention and Control of Pneumonia and Diarrhea (GAPPD) in 2013, aiming at significantly reducing the incidence of childhood pneumonia by promoting proper nutrition, vaccination, hygiene, adequate breastfeeding, timely treatment of associated illnesses, and ensuring access to proper healthcare [14].

To diagnose pneumonia, healthcare providers typically begin by reviewing the patient's medical history and conducting a physical examination, including listening to the lungs with a stethoscope. Additional diagnostic procedures may include chest imaging, such as x-rays, pulse oximetry to assess blood oxygen levels, and laboratory tests of blood or sputum samples to identify the causative organism [15]. Pneumonia treatment differs according to the identified causative agent, and amoxicillin is generally used as the primary therapy, administered twice per day for a duration of 3–5 days [16]. While clotrimazole is available as an alternative treatment, treatment failure may occur, necessitating hospital care for children who exhibit no improvement in respiratory rate within 48–72 h of therapy [16].

Vaccination remains the most effective strategy for preventing pneumococcal pneumonia [17]. Pneumococcal vaccines are widely utilized to prevent pneumococcal pneumonia and are categorized into two main types: pneumococcal polysaccharide vaccines (PPSVs) and pneumococcal conjugate vaccines (PCVs). The PPSV group includes the 23-valent pneumococcal polysaccharide vaccine (PPSV23), which targets 23 serotypes. The PCV group consists of protein-conjugated vaccines such as PCV13, PCV15, and PCV20, which protect against 13, 15, and 20 serotypes, respectively [18]. PCVs are recommended for infants and children younger than 5 years old, whereas PPSV23 is recommended for individuals aged 65 and older, as well as those over 5 years old who have an elevated risk of developing pneumococcal infection [19, 20]. However, challenges remain because some children carry multiple serotypes of *Streptococcus pneumoniae*, which reduces their responsiveness to vaccination. This situation complicates pneumonia transmission dynamics as vaccinated individuals may still act as sources of infection [21, 22].

Mathematical modeling of infectious diseases has become an indispensable tool for understanding and predicting the spread of infections, assessing their impact on populations, and helping to develop strategies for controlling outbreaks [23, 24]. Among the various modeling approaches, reaction-diffusion systems have proven to be effective and suitable modeling tools for understanding the spatial temporal dynamics of disease transmission [25]. These models describe disease dynamics through two fundamental mechanisms: reaction, which represents local interactions among individuals, and diffusion, which governs the spatial movements of individuals [26]. Such spatial epidemic models have been employed to investigate the propagation, persistence, and asymptotic dynamics of infectious diseases, particularly in heterogeneous environments [27–30]. Spatial propagation has also been investigated through traveling-wave approaches, which provide insights into the conditions required for infections to spread through space [31]. These systems have been utilized across numerous fields, including physics, chemistry, and biology, to model processes such as wave propagation, chemical reactions, and biological pattern formation [32]. Unlike traditional models which are based on ordinary differential equations (ODEs) having only the dimension of time, reaction-diffusion systems employ partial differential equations (PDEs), incorporating both time and space dimensions to accurately capture spatial variations [33, 34].

Despite the progress in modeling pneumonia, existing studies, such as [1, 3, 7–9, 21, 35, 36], among others, have largely focused on temporal dynamics, with limited attention to how infection spreads and persists across space. Addressing this gap is essential for developing more realistic insights into disease behavior and informing targeted control strategies. This study therefore examines the combined effects of spatial–temporal variations, treatment, and vaccination interventions on pneumococcal pneumonia transmission, offering insights not captured in earlier works.

2 | Model Formulation

The model consists of 5 compartments representing the population densities of Susceptible individuals $S(x,t)$ who are at risk of the infection, Asymptomatic infectious individuals $C(x,t)$, Symptomatic infectious individuals $I(x,t)$, individuals who have recovered from the disease $R(x,t)$, and Vaccinated individuals $V(x,t)$. The total population density is given by

$$N(x,t) = S(x,t) + C(x,t) + I(x,t) + R(x,t) + V(x,t).$$

2.1 | Model Assumptions

1. Recruitment is strictly into the susceptible at constant rate Λ.
2. Recovered individuals who do not receive vaccination become susceptible again.
3. There are individuals who do not react to the vaccine.

4. The vaccine gives permanent immunity in the presence of booster doses.
5. Recovery is through treatment.

2.2 | Model Parameters

See Table 1.

2.3 | Compartmental Diagram of the Model

See Figure 1.

2.4 | Equations of the Model

We assume that the population moves in the region Ω according to Fick's law [40]. Each diffusion coefficient d_i $(i = 1, \ldots, 5)$ determines the rate at which each sub population disperses throughout space. The Laplacian operator Δ represents the spatial diffusion of the disease between neighboring locations. This together with Figure 1 give the following system

TABLE 1 | Description and values of model parameters.

Parameter	Description	Value/day	Source
Λ	Constant recruitment rate	11	Assumed
τ_1	Rate at which susceptibles are vaccinated	0.008	[36]
k	Contact rate with either a carrier or infected individual	1–10	[37]
p	Likelihood that a contact is sufficient to induce infection	0.89–0.99	[36]
ω	Transmission coefficient of carriers	0.41026	[38]
α	Progression rate from C to I	0.01096	[8]
γ	Recovery rate of infected individuals	0.0115	[39]
π	Recovery rate of carriers	0.0076	[39]
τ_2	Rate at which recovered individuals are vaccinated	0.2	Assumed
θ	Rate at which recovered become susceptible again	0.0241	[8]
μ	Natural death rate per individual	0.0002	[35]
ε	Disease-induced death rate	0.1	[7]
ϕ	Proportion of susceptibles who become carriers upon infection	0.338	[8]
ξ	Rate at which individuals do not respond to the vaccine	0.002	[39]
σ	Proportion of vaccinated individuals who become carriers upon infection	0.2	[39]

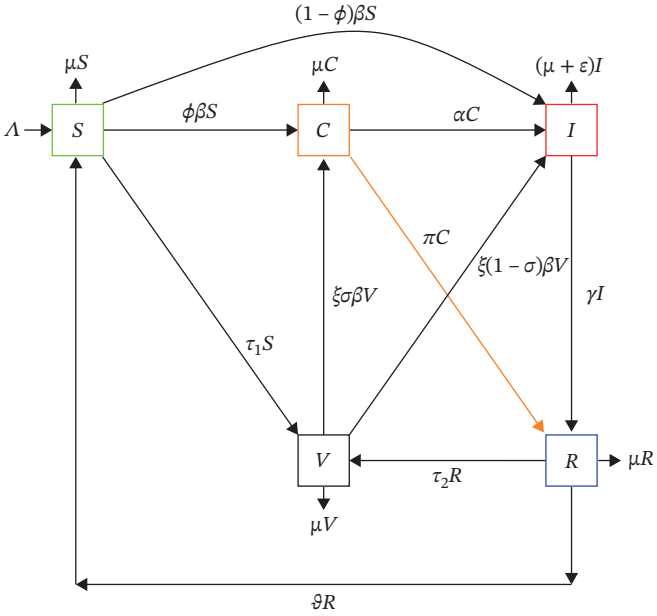


FIGURE 1 | A compartmental diagram showing the transmission dynamics of pneumococcal pneumonia.

$$\begin{aligned}
\frac{\partial S(x,t)}{\partial t} &= d_1\Delta S + \Lambda + \theta R - \tau_1 S - \mu S - \beta S,\\
\frac{\partial C(x,t)}{\partial t} &= d_2\Delta C + \phi\beta S + \xi\sigma\beta V - (\mu+\alpha+\pi)C,\\
\frac{\partial I(x,t)}{\partial t} &= d_3\Delta I + (1-\phi)\beta S + \alpha C + \xi(1-\sigma)\beta V - (\mu+\varepsilon+\gamma)I,\\
\frac{\partial R(x,t)}{\partial t} &= d_4\Delta R + \pi C + \gamma I - (\mu+\theta+\tau_2)R,\\
\frac{\partial V(x,t)}{\partial t} &= d_5\Delta V + \tau_1 S + \tau_2 R - \mu V - \xi\beta V.
\end{aligned} \tag{1}$$

Susceptible individuals acquire pneumonia upon contact with infected or carrier individuals by the force of infection

$$\beta = \eta\left(\frac{I+\omega C}{N}\right), \tag{2}$$

where $\eta = kp$ is the transmission rate.

System (1) is subjected to initial conditions:

$S(x,0) = S_0(x)$, $C(x,0) = C_0(x)$, $I(x,0) = I_0(x)$, $R(x,0) = R_0(x)$, and $V(x,0) = V_0(x), x \in \Omega$ together with homogeneous Neumann boundary conditions

$$\begin{aligned}
&\frac{\partial S(x,t)}{\partial n} = \frac{\partial C(x,t)}{\partial n} = \frac{\partial I(x,t)}{\partial n} = \frac{\partial R(x,t)}{\partial n}\\
&= \frac{\partial V(x,t)}{\partial n} = 0,\ x \in \partial\Omega,\ t > 0,
\end{aligned} \tag{3}$$

where Ω is a bounded domain of $\mathbb{R}^5$ with smooth boundary $\partial\Omega$, and n is the unit outer vector normal to the boundary, $\partial\Omega$.

3 | Analysis of the Model

3.1 | Positivity and Boundedness of the Solutions

Lemma 1. *For $t>0$ and $x\in\Omega$, the solutions $S(x,t)$, $C(x,t)$, $I(x,t)$, $R(x,t)$ and $V(x,t)$ of the system (1) are non-negative.*

Proof. Assume that the initial conditions are non-negative, that is,

$$S(x,0)\geq 0,\ C(x,0)\geq 0,\ I(x,0)\geq 0,$$
$$R(x,0)\geq 0,\ V(x,0)\geq 0,\ \forall x\in\Omega.$$

We aim to prove that the solutions of the system remain non-negative for all $t>0$. Observe that each reaction term is quasi-positive.

Consider

$$\frac{\partial S}{\partial t}=d_1\Delta S+\Lambda+\theta R-\tau_1 S-\mu S-\beta S. \tag{4}$$

Suppose, by contradiction, that there exists $t_s>0$ and $x_s\in\Omega$ at which $S(x_s,t_s)=0$, $\frac{\partial S}{\partial t}\leq 0$ and $\Delta S\geq 0$. Then evaluating (4) at this point $S(x_s,t_s)=0$, the reaction terms become $\Lambda+\theta R\geq 0$ and so

$$\frac{\partial S}{\partial t}=d_1\Delta S+\Lambda+\theta R\geq 0,$$

which contradicts $\frac{\partial S}{\partial t}(x_s,t_s)\leq 0$. Therefore, S cannot attain a negative minimum in the interior of Ω. If a negative minimum were attained at the boundary, Hopf's boundary point lemma would imply $\frac{\partial S}{\partial n}<0$, which contradicts the homogeneous Neumann boundary condition, $\partial S/\partial n=0$ on $\partial\Omega$. Hence, by the strong maximum principle together with Hopf's lemma [41], we conclude that $S(x,t)\geq 0$ for all $x\in\Omega,\ t>0$. Similarly, for the carrier class,

$$\frac{\partial C}{\partial t}=d_2\Delta C+\phi\beta S+\xi\sigma\beta V-(\mu+\alpha+\pi)C. \tag{5}$$

Also suppose that there exist $t_c>0$ and $x_c\in\Omega$ such that $C(x_c,t_c)=0$ and C attains a negative minimum at (x_c,t_c). Then at this point $\frac{\partial C}{\partial t}(x_c,t_c)\leq 0,\ \Delta C(x_c,t_c)\geq 0$. Using $\beta=\eta(\frac{I+\omega C}{N})$, when $C=0$, the reaction terms in (5) become $\frac{\eta I}{N}(\phi S+\xi\sigma V)\geq 0$. Thus

$$\frac{\partial C}{\partial t}=d_2\Delta C+\frac{\eta I}{N}(\phi S+\xi\sigma V)\geq 0.$$

Applying the same argument yields $C(x,t)\geq 0$.

For the infected class,

$$\frac{\partial I}{\partial t}=d_3\Delta I+(1-\phi)\beta S+\alpha C+\xi(1-\sigma)\beta V-(\mu+\varepsilon+\gamma)I. \tag{6}$$

Suppose that also at some time $t_i>0$ and $x_i\in\Omega$ such that $I(x_i,t_i)=0$ and I attains a negative minimum at (x_i,t_i). Then at this point $\frac{\partial I}{\partial t}(x_i,t_i)\leq 0,\ \Delta I(x_i,t_i)\geq 0$. At this point, the reaction terms in (6) reduce to $\frac{\eta\omega C}{N}((1-\phi)S+\xi(1-\sigma)V)+\alpha C\geq 0$ and so

$$\frac{\partial I}{\partial t}=d_3\Delta I+\frac{\eta\omega C}{N}((1-\phi)S+\xi(1-\sigma)V)+\alpha C\geq 0.$$

Also by applying strong maximum principle and Hopf's Lemma, $I(x,t)\geq 0$.

For the recovered class,

$$\frac{\partial R}{\partial t}=d_4\Delta R+\pi C+\gamma I-(\mu+\theta+\tau_2)R. \tag{7}$$

Likewise, suppose that at some time $t_r>0$, $R(x_r,t_r)=0$. R attains a negative minimum at (x_r,t_r). Then the reaction terms in(7) become $\pi C+\gamma I\geq 0$ and therefore

$$\frac{\partial R}{\partial t}=d_4\Delta R+\pi C+\gamma I\geq 0.$$

By applying strong maximum principle and Hopf's Lemma, $R(x,t)\geq 0$.

Now, consider

$$\frac{\partial V(x,t)}{\partial t}=d_5\Delta V+\tau_1 S+\tau_2 R-\mu V-\xi\beta V. \tag{8}$$

Suppose that at some time $t_v>0$, and $x_v\in\Omega$ such that $V(x_v,t_v)=0$ and V attains a negative minimum at (x_v,t_v). Then at this point $\frac{\partial V}{\partial t}(x_v,t_v)\leq 0,\ \Delta V(x_v,t_v)\geq 0$. Then the reaction terms in (8) reduce to $\tau_1 S+\tau_2 R\geq 0$ so that

$$\frac{\partial V}{\partial t}=d_5\Delta V+\tau_1 S+\tau_2 R\geq 0.$$

By applying strong maximum principle and Hopf's Lemma, $V(x,t)\geq 0$.

Consequently $S(x,t)\geq 0,\ C(x,t)\geq 0,\ I(x,t)\geq 0,\ R(x,t)\geq 0$ and $V(x,t)\geq 0$ for all $x\in\Omega$ and $t>0$. □

Lemma 2. *The solutions of the system (1) remain uniformly bounded for all time $t>0$ and $x\in\Omega$.*

Proof. To establish the uniform boundedness of the system, we define the total population density at location x and time t as

$$N(x,t)=S(x,t)+C(x,t)+I(x,t)+R(x,t)+V(x,t).$$

Differentiating $N(x,t)$ with respect to time and substituting for the model equations in (1), we obtain

$$\frac{\partial N}{\partial t}=d_1\Delta S+d_2\Delta C+d_3\Delta I+d_4\Delta R+d_5\Delta V+\Lambda-\mu N-\varepsilon I. \tag{9}$$

Integrating (9) over the spatial domain Ω and applying homogeneous Neumann boundary conditions (3), the diffusion terms vanish, giving

$$\frac{d}{dt}\int_\Omega N(x,t)\,dx=\Lambda|\Omega|-\mu\int_\Omega N(x,t)\,dx-\varepsilon\int_\Omega I(x,t)\,dx.$$

From which

$$\frac{d}{dt}\int_{\Omega} N(x,t)\,dx \le \Lambda|\Omega| - \mu\int_{\Omega} N(x,t)\,dx, \tag{10}$$

where $|\Omega|$ denotes the Lebesgue measure of Ω. Letting

$$Y(t) = \int_{\Omega} N(x,t)\,dx, \tag{11}$$

the inequality (10) becomes

$$Y'(t) + \mu Y(t) \le \Lambda|\Omega|. \tag{12}$$

Using the initial condition $Y(0) = Y_0$, we integrate (12) to obtain

$$Y(t) \le \frac{\Lambda|\Omega|}{\mu} + \left(Y_0 - \frac{\Lambda|\Omega|}{\mu}\right)e^{-\mu t}.$$

Taking the limit as $t \to \infty$, we have

$$\lim_{t\to\infty} Y(t) \le \frac{\Lambda|\Omega|}{\mu}.$$

Hence from (11), we have

$$\lim_{t\to\infty}\int_{\Omega} N(x,t)\,dx \le \frac{\Lambda|\Omega|}{\mu}.$$

Since

$$S(x,t) \le N(x,t),\ C(x,t) \le N(x,t),\ I(x,t) \le N(x,t),$$
$$R(x,t) \le N(x,t),\ V(x,t) \le N(x,t),$$

it follows that all state variables are uniformly bounded. □

3.2 | Disease-Free Equilibrium

This exists in the absence of the disease, implying that the carrier population C and the infected population I are both zero. Consequently, the number of recovered individuals R also becomes zero, that is, $C = I = R = 0$. Setting the right-hand sides of system (1) to zero and solving for S and V, we get $S = \frac{\Lambda}{\tau_1+\mu}$ and $V = \frac{\tau_1\Lambda}{\mu(\tau_1+\mu)}$. Thus, the disease free equilibrium point is $E_0 = (\frac{\Lambda}{\tau_1+\mu}, 0, 0, 0, \frac{\tau_1\Lambda}{\mu(\tau_1+\mu)})$.

3.3 | Effective Reproduction Number

According to Watmough and Van den Driessche [42], the basic reproduction number, denoted by, $\mathscr{R}_0$, is the average number of secondary infections that occur when one infective individual is introduced into completely susceptible population. When control interventions are introduced into the model, the corresponding transmission potential is described by the effective reproduction number, denoted by $\mathscr{R}_e$, which accounts for the effect of these interventions on disease transmission [43]. In this study, effective reproduction number, $\mathscr{R}_e$, refers to the average number of new pneumonia infections generated by a single infectious individual introduced into a fully susceptible population in presence of vaccination. It is obtained using the next-generation matrix method [42], and mathematically, it is the spectral radius of the next-generation matrix. This approach has also been employed in [21, 26, 44].

To compute the effective reproduction number, the infected compartments (C, I) of the system are considered,

$$\begin{aligned}\frac{\partial C(x,t)}{\partial t} &= d_2\Delta C + \phi\beta S + \xi\sigma\beta V - (\mu+\alpha+\pi)C,\\ \frac{\partial I(x,t)}{\partial t} &= d_3\Delta I + (1-\phi)\beta S + \alpha C + \xi(1-\sigma)\beta V - (\mu+\varepsilon+\gamma)I.\end{aligned} \tag{13}$$

The nonspatial component of system (13) is considered, since $\mathscr{R}_e$ is typically derived from the local dynamics at the disease-free equilibrium, ignoring diffusion. The matrices F_i and V_i, representing the rates new infections and movement rates between the compartments, respectively, are then constructed.

$$F_i = \begin{bmatrix} \phi\beta S + \xi\sigma\beta V \\ (1-\phi)\beta S + \xi(1-\sigma)\beta V \end{bmatrix}, \quad V_i = \begin{bmatrix} (\alpha+\mu+\pi)C \\ (\mu+\varepsilon+\gamma)I - \alpha C \end{bmatrix}. \tag{14}$$

By evaluating the Jacobian matrices of F_i and V_i in (14) at the disease-free equilibrium E_0, the following matrices are obtained.

$$F = \begin{bmatrix} \frac{\eta\omega}{\tau_1+\mu}(\phi\mu + \xi\sigma\tau_1) & \frac{\eta}{\tau_1+\mu}(\phi\mu + \xi\sigma\tau_1) \\ \frac{\eta\omega}{\tau_1+\mu}((1-\phi)\mu + \xi(1-\sigma)\tau_1) & \frac{\eta}{\tau_1+\mu}((1-\phi)\mu + \xi(1-\sigma)\tau_1) \end{bmatrix}, \tag{15}$$

$$V = \begin{bmatrix} k_1 & 0 \\ -\alpha & k_2 \end{bmatrix}, \tag{16}$$

where $k_1 = \mu+\alpha+\pi$ and $k_2 = \mu+\varepsilon+\gamma$. Using matrices (15) and (16), the next-generation matrix FV^{-1} is derived as

$$\begin{bmatrix} \frac{\eta\omega}{k_1(\tau_1+\mu)}(\phi\mu + \xi\sigma\tau_1) + \frac{\eta\alpha}{k_1k_2(\tau_1+\mu)}(\phi\mu + \xi\sigma\tau_1) & \frac{\eta}{k_2(\tau_1+\mu)}(\phi\mu + \xi\sigma\tau_1) \\ \frac{\eta\omega}{k_1(\tau_1+\mu)}((1-\phi)\mu + \xi(1-\sigma)\tau_1) + \frac{\eta\alpha}{k_1k_2(\tau_1+\mu)}((1-\phi)\mu + \xi(1-\sigma)\tau_1) & \frac{\eta}{k_2(\tau_1+\mu)}((1-\phi)\mu + \xi(1-\sigma)\tau_1) \end{bmatrix}.$$

$$FV^{-1} = \frac{\eta}{k_1 k_2(\tau_1+\mu)} \begin{bmatrix} (\phi\mu + \xi\sigma\tau_1)(k_2\omega+\alpha) & k_1(\phi\mu+\xi\sigma\tau_1) \\ ((1-\phi)\mu + \xi(1-\sigma)\tau_1)(k_2\omega+\alpha) & k_1((1-\phi)\mu+\xi(1-\sigma)\tau_1) \end{bmatrix}. \tag{17}$$

Thus, the eigenvalues of the matrix (17) are $\lambda_1 = 0$ and $\lambda_2 = \frac{\eta}{k_1 k_2(\tau_1+\mu)}((\phi\mu+\xi\sigma\tau_1)(k_2\omega+\alpha) + k_1((1-\phi)\mu+\xi(1-\sigma)\tau_1))$. According to [45] the dominant eigenvalue of the matrix (17) yields the effective reproduction number,

$$\begin{aligned} \mathscr{R}_e = \frac{\eta}{k_1 k_2(\tau_1+\mu)}&[(\phi\mu+\xi\sigma\tau_1)(k_2\omega+\alpha) \\ &+ k_1((1-\phi)\mu+\xi(1-\sigma)\tau_1)]. \end{aligned} \tag{18}$$

In absence of vaccination, that is, when $\tau_1 = 0$, the basic reproduction number, $\mathscr{R}_0$, is obtained as

$$\mathscr{R}_0 = \frac{\eta}{k_1 k_2}[\phi(k_2\omega+\alpha) + k_1(1-\phi)]. \tag{19}$$

Accordingly, the efective reproduction number can be expressed in terms of the basic reproduction number as

$$\mathscr{R}_e = \frac{1}{\tau_1+\mu}\left[\mu\mathscr{R}_0 + \frac{\eta\xi\tau_1}{k_1 k_2}(\sigma(k_2\omega+\alpha) + k_1(1-\sigma))\right]. \tag{20}$$

3.4 | Local Stability of the Disease-Free Equilibrium

To investigate the local stability of the equilibrium point, we use a similar approach as applied in [25, 26]. We start by defining some of the necessary notations and definitions. Consider the Laplacian operator $-\Delta$ on the domain Ω with Neumann boundary conditions. Its eigenvalues form an infinite, ordered sequence $0 = \lambda_0 < \lambda_1 < \lambda_2 < \cdots$, where each eigenvalue λ_i has an algebraic multiplicity $m_i \geq 1$. The normalized eigenfunctions associated with λ_i are represented as Φ_{ij} for $j = 1, 2, \ldots, m_i$. Notably as $i \to \infty$, the eigenvalues $\lambda_i \to \infty$, and that the corresponding eigenfunction Φ_0 is constant. Also, from standard eigenfunction theory,

$$\begin{aligned} -\Delta\Phi_{ij} &= \lambda_i\Phi_{ij}, \quad \text{in } \Omega, \\ \frac{\partial\Phi_{ij}}{\partial n} &= 0, \quad \text{on } \partial\Omega. \end{aligned}$$

The eigenfunctions are normalized according to equation (21)

$$\int_\Omega \Phi_{ij}^2(x)dx = 1. \tag{21}$$

Consequently, the collection $\{\Phi_{ij} : 1 \leq j \leq m_i\}$ forms an orthonormal and complete basis. In general, system (1) can be expressed as a two component reaction-diffusion model of the form

$$\frac{\partial U}{\partial t} = \mathrm{JU} + D\Delta U,$$

where $D = \mathrm{diag}(d_1, d_2, d_3, d_4, d_5)$ is a diagonal matrix of diffusion coefficients, $U = (S, C, I, R, V)^T$ and J is the Jacobian matrix derived from the reaction terms of the corresponding system of ODEs. More explicitly,

$$\begin{aligned} \frac{\partial U}{\partial t} = &\begin{bmatrix} -(\tau_1+\mu+\beta) & -\eta\omega\frac{S}{N} & -\eta\frac{S}{N} & \theta & 0 \\ \phi\beta & A_{22}-k_1 & A_{23} & 0 & \xi\sigma\beta \\ (1-\phi)\beta & A_{32} & A_{33}-k_2 & 0 & \xi(1-\sigma)\beta \\ 0 & \pi & \gamma & -k_3 & 0 \\ \tau_1 & -\xi\eta\omega\frac{V}{N} & -\xi\eta\frac{V}{N} & \tau_2 & -\mu-\xi\beta \end{bmatrix} U \\ &+ \begin{bmatrix} d_1 & 0 & 0 & 0 & 0 \\ 0 & d_2 & 0 & 0 & 0 \\ 0 & 0 & d_3 & 0 & 0 \\ 0 & 0 & 0 & d_4 & 0 \\ 0 & 0 & 0 & 0 & d_5 \end{bmatrix} \Delta U. \end{aligned} \tag{22}$$

Consequently, the reaction-diffusion system can be written as

$$\frac{\partial U}{\partial t} = \begin{bmatrix} d_1\Delta - (\tau_1+\mu+\beta) & -\eta\omega\frac{S}{N} & -\eta\frac{S}{N} & \theta & 0 \\ \phi\beta & d_2\Delta + A_{22} - k_1 & A_{23} & 0 & \xi\sigma\beta \\ (1-\phi)\beta & A_{32} & d_3\Delta + A_{33} - k_2 & 0 & \xi(1-\sigma)\beta \\ 0 & \pi & \gamma & d_4\Delta - k_3 & 0 \\ \tau_1 & -\xi\eta\omega\frac{V}{N} & -\xi\eta\frac{V}{N} & \tau_2 & d_5\Delta - \mu - \xi\beta \end{bmatrix} U,$$

where

$$
\begin{aligned}
k_1 &= \mu + \alpha + \pi,\\
k_2 &= \mu + \varepsilon + \gamma,\\
k_3 &= \mu + \theta + \tau_2,\\
A_{22} &= \phi\eta\omega\frac{S}{N} + \xi\sigma\eta\omega\frac{V}{N},\\
A_{23} &= \phi\eta\frac{S}{N} + \xi\sigma\eta\frac{V}{N},\\
A_{32} &= (1-\phi)\eta\omega\frac{S}{N} + \alpha + \xi(1-\sigma)\eta\omega\frac{V}{N},\\
A_{33} &= (1-\phi)\eta\frac{S}{N} + \xi(1-\sigma)\eta\frac{V}{N}.
\end{aligned}
$$

The corresponding linearizing operator acting on U is therefore given by

$$
\mathscr{L} = \begin{bmatrix}
d_1\Delta - (\tau_1 + \mu + \beta) & -\eta\omega\dfrac{S}{N} & -\eta\dfrac{S}{N} & \theta & 0\\
\phi\beta & d_2\Delta + A_{22} - k_1 & A_{23} & 0 & \xi\sigma\beta\\
(1-\phi)\beta & A_{32} & d_3\Delta + A_{33} - k_2 & 0 & \xi(1-\sigma)\beta\\
0 & \pi & \gamma & d_4\Delta - k_3 & 0\\
\tau_1 & -\xi\eta\omega\dfrac{V}{N} & -\xi\eta\dfrac{V}{N} & \tau_2 & d_5\Delta - \mu - \xi\beta
\end{bmatrix}.
$$

Thus, let J_i denote the Jacobian matrix of the system (1) and it is given by

$$
J_i = \begin{bmatrix}
-d_1\lambda_i - (\tau_1 + \mu + \beta) & -\eta\omega\dfrac{S}{N} & -\eta\dfrac{S}{N} & \theta & 0\\
\phi\beta & -d_2\lambda_i + A_{22} - k_1 & A_{23} & 0 & \xi\sigma\beta\\
(1-\phi)\beta & A_{32} & -d_3\lambda_i + A_{33} - k_2 & 0 & \xi(1-\sigma)\beta\\
0 & \pi & \gamma & -d_4\lambda_i - k_3 & 0\\
\tau_1 & -\xi\eta\omega\dfrac{V}{N} & -\xi\eta\dfrac{V}{N} & \tau_2 & -d_5\lambda_i - \mu - \xi\beta
\end{bmatrix}. \tag{23}
$$

Theorem 1. *The disease free equilibrium E_0 of the system (1) is locally asymptotically stable if $\mathscr{R}_e < 1$.*

Proof. Evaluating (23) at E_0, leads to

$$
J_i(E_0) = \begin{bmatrix}
-\lambda_i d_1 - \tau_1 - \mu & -\eta\omega\dfrac{\mu}{\tau_1+\mu} & -\eta\dfrac{\mu}{\tau_1+\mu} & \theta & 0\\
0 & -\lambda_i d_2 - k_1 + A_{22} & A_{23} & 0 & 0\\
0 & A_{32} & -\lambda_i d_3 - k_2 + A_{33} & 0 & 0\\
0 & \pi & \gamma & -\lambda_i d_4 - k_3 & 0\\
\tau_1 & -\xi\eta\omega\dfrac{\tau_1}{\tau_1+\mu} & -\xi\eta\dfrac{\tau_1}{\tau_1+\mu} & \tau_2 & -\lambda_i d_5 - \mu
\end{bmatrix}, \tag{24}
$$

where

$$
\begin{aligned}
A_{22} &= \phi\eta\omega\frac{\mu}{\tau_1+\mu} + \xi\sigma\eta\omega\frac{\tau_1}{\tau_1+\mu},\\
A_{23} &= \phi\eta\frac{\mu}{\tau_1+\mu} + \xi\sigma\eta\frac{\tau_1}{\tau_1+\mu},\\
A_{32} &= (1-\phi)\eta\omega\frac{\mu}{\tau_1+\mu} + \alpha + \xi(1-\sigma)\eta\omega\frac{\tau_1}{\tau_1+\mu},\\
A_{33} &= (1-\phi)\eta\frac{\mu}{\tau_1+\mu} + \xi(1-\sigma)\eta\frac{\tau_1}{\tau_1+\mu}.
\end{aligned}
$$

From (24), it is clear that, $-(\lambda_i d_5 + \mu)$, $-(\lambda_i d_1 + \tau_1 + \mu)$, and $-(\lambda_i d_4 + k_3)$ are negative eigenvalues. It remains to examine the remaining stability conditions. After accounting for the eigenvalues already determined, the Jacobian matrix (24) reduces to the following 2×2 form

$$
J_i'(E_0) = \begin{bmatrix}
-\lambda_i d_2 - k_1 + A_{22} & A_{23}\\
A_{32} & -\lambda_i d_3 - k_2 + A_{33}
\end{bmatrix}.
$$

Applying the trace–determinant criterion to $J_i'(E_0)$, we obtain the trace as

$$tr\,(J_i'(E_0)) = -(\lambda_i(d_2+d_3)+k_1+k_2-A_{22}-A_{33})<0,$$

and determinant as

$$\begin{aligned}\det(J_i'(E_0)) = {} & k_1k_2(1-\mathscr{R}_e)+\lambda_i^2 d_2d_3\\ & +\lambda_i d_2\left[\frac{k_2(\tau_1+\mu)-\eta((1-\phi)\mu+\xi(1-\sigma)\tau_1)}{\tau_1+\mu}\right]\\ & +\lambda_i d_3\left[\frac{k_1(\tau_1+\mu)-\eta\omega(\phi\mu+\xi\sigma\tau_1)}{\tau_1+\mu}\right]>0,\end{aligned}$$

whenever $\mathscr{R}_e<1$.

Since $tr(J_i'(E_0))<0$ and $\det(J_i'(E_0))>0$ whenever $\mathscr{R}_e<1$, the disease-free equilibrium E_0 is locally asymptotically stable for $\mathscr{R}_e<1$. □

3.5 | Global Stability of the Disease-Free Equilibrium

Theorem 2. *The disease free equilibrium, E_0 is globally asymptotically stable if $\mathscr{R}_e<1$ and unstable if $\mathscr{R}_e>1$.*

Proof. Consider a Lyapunov function of the form

$$L=\int_\Omega[\Psi_1C(x,t)+\Psi_2I(x,t)]dx, \tag{25}$$

where Ψ_1 and Ψ_2 are positive constants. Taking the time derivative of L in (25) yields

$$\frac{dL}{dt}=\int_\Omega\left[\Psi_1\frac{\partial C(x,t)}{\partial t}+\Psi_2\frac{\partial I(x,t)}{\partial t}\right]dx. \tag{26}$$

Substituting the expressions for $\frac{\partial C(x,t)}{\partial t}$ and $\frac{\partial I(x,t)}{\partial t}$ into (26) gives

$$\begin{aligned}\frac{dL}{dt} = {} & \int_\Omega[\Psi_1(d_2\Delta C+\phi\beta S+\xi\sigma\beta V-(\mu+\alpha+\pi)C)\\ & +\Psi_2(d_3\Delta I+(1-\phi)\beta S+\alpha C\\ & +\xi(1-\sigma)\beta V-(\mu+\varepsilon+\gamma)I)]dx.\end{aligned}$$

Upon substituting for $\beta=\eta(\frac{I+\omega C}{N})$ and expanding the infection terms, we obtain

$$\begin{aligned}\frac{dL}{dt}=\int_\Omega\Bigg[& \left(\Psi_1\left(\phi\eta\omega\frac{S}{N}+\xi\sigma\eta\omega\frac{V}{N}-k_1\right)\right.\\ & \left.+\Psi_2\left((1-\phi)\eta\omega\frac{S}{N}+\alpha+\xi(1-\sigma)\eta\omega\frac{V}{N}\right)\right)C\\ & +\left(\Psi_1\left(\phi\eta\frac{S}{N}+\xi\sigma\eta\frac{V}{N}\right)\right.\\ & \left.+\Psi_2\left((1-\phi)\eta\frac{S}{N}+\xi(1-\sigma)\eta\frac{V}{N}-k_2\right)\right)I\Bigg]dx\\ & +\int_\Omega[\Psi_1d_2\Delta C+\Psi_2d_3\Delta I]dx.\end{aligned} \tag{27}$$

Using Green's formula together with Neumann boundary conditions (3), we obtain

$$\int_\Omega[\Psi_1d_2\Delta C+\Psi_2d_3\Delta I]dx=0.$$

Thus, (27) becomes,

$$\begin{aligned}\frac{dL}{dt} = {} & \int_\Omega\left[\left(\Psi_1\left(\phi\eta\omega\frac{S}{N}+\xi\sigma\eta\omega\frac{V}{N}-k_1\right)+\Psi_2\left((1-\phi)\eta\omega\frac{S}{N}+\alpha+\xi(1-\sigma)\eta\omega\frac{V}{N}\right)\right)C\right.\\ & \left.+\left(\Psi_1\left(\phi\eta\frac{S}{N}+\xi\sigma\eta\frac{V}{N}\right)+\Psi_2\left((1-\phi)\eta\frac{S}{N}+\xi(1-\sigma)\eta\frac{V}{N}-k_2\right)\right)I\right]dx.\end{aligned}$$

Applying the values of $\frac{S}{N}=\frac{\mu}{\tau_1+\mu}$ and $\frac{V}{N}=\frac{\tau_1}{\tau_1+\mu}$ at disease free equilibrium gives

$$\begin{aligned}\frac{dL}{dt} = {} & \int_\Omega\left[\left(\Psi_1\left(\frac{\phi\eta\omega\mu+\xi\sigma\eta\omega\tau_1-k_1(\tau_1+\mu)}{(\tau_1+\mu)}\right)+\Psi_2\left(\frac{(1-\phi)\eta\omega\mu+\alpha(\tau_1+\mu)+\xi(1-\sigma)\eta\omega\tau_1}{(\tau_1+\mu)}\right)\right)C\right.\\ & \left.+\left(\Psi_1\left(\frac{\phi\eta\mu+\xi\sigma\eta\tau_1}{\tau_1+\mu}\right)+\Psi_2\left(\frac{(1-\phi)\eta\mu+\xi(1-\sigma)\eta\tau_1-k_2(\tau_1+\mu)}{\tau_1+\mu}\right)\right)I\right]dx.\end{aligned}$$

Setting

$$\Psi_2=\frac{(k_1(\tau_1+\mu)-\xi\sigma\eta\omega\tau_1-\phi\eta\omega\mu)\Psi_1}{(1-\phi)\eta\omega\mu+\alpha(\tau_1+\mu)+\xi(1-\sigma)\eta\omega\tau_1},$$

and $\Psi_1>0$, it follows that

$$\frac{dL}{dt}=\Psi_1\int_\Omega\left[\frac{k_1k_2(\tau_1+\mu)}{(1-\phi)\eta\omega\mu+\alpha(\tau_1+\mu)+\xi(1-\sigma)\eta\omega\tau_1}(\mathscr{R}_e-1)\right]Idx.$$

Therefore, $\frac{dL}{dt}<0$ whenever $\mathscr{R}_e<1$ and otherwise $\frac{dL}{dt}>0$ when $\mathscr{R}_e>1$. Also note that $\frac{dL}{dt}=0$ only when either $I=0$ or $\mathscr{R}_e=1$. In either case, the largest compact invariant set in $\{(S,C,I,R,V)\in\Omega|\frac{dL}{dt}=0\}$ is the singleton E_0. By Lasalle's invariant principle in [46], this implies that E_0 is globally asymptotically stable in Ω if $\mathscr{R}_e<1$ and unstable if $\mathscr{R}_e>1$. □

3.6 | Endemic Equilibrium

Endemic equilibrium occurs when pneumococcal pneumonia persists in the population and we shall denote it by $E_e = (S^*, C^*, I^*, R^*, V^*)$. In order to determine the endemic equilibrium point, we equate the reaction part of the system (1) to zero, that is,

$$\begin{aligned} \Lambda + \theta R - (\tau_1 + \mu + \beta)S &= 0, \\ \phi\beta S + \xi\sigma\beta V - k_1 C &= 0, \\ (1-\phi)\beta S + \alpha C + \xi(1-\sigma)\beta V - k_2 I &= 0, \\ \pi C + \gamma I - k_3 R &= 0, \\ \tau_1 S + \tau_2 R - \mu V - \xi\beta V &= 0. \end{aligned} \tag{28}$$

Solving system (28) together with

$$\Lambda - \mu N^* - \varepsilon I = 0,$$

and

$$\beta = \eta\left(\frac{I + \omega C}{N^*}\right), \text{ where } N^* \text{ is the total population at equilibrium .}$$

The endemic equilibrium state E_e is given by

$$\begin{aligned} S^* &= \frac{N^*[\Lambda(\varepsilon k_3 + \theta\gamma) + \theta\varepsilon\pi C^* - \theta\gamma\mu N^*]}{k_3[\varepsilon N^*(\tau_1 + \mu) + \eta(\Lambda - \mu N^* + \varepsilon\omega C^*)]}, \\ C^* &= \frac{-b' + \sqrt{(b')^2 - 4a'c'}}{2a'}, \\ I^* &= \frac{\Lambda - \mu N^*}{\varepsilon}, \\ R^* &= \frac{\varepsilon\pi C^* + \gamma(\Lambda - \mu N^*)}{\varepsilon k_3}, \\ V^* &= \frac{N^*[\varepsilon\tau_1 N^* Y + \tau_2(\varepsilon\pi C^* + \gamma(\Lambda - \mu N^*))Z]}{k_3 Z(\mu\varepsilon N^* + \xi\eta X)}, \end{aligned}$$

where

$$\begin{aligned} &X = \Lambda - \mu N^* + \varepsilon\omega C^*,\ Y = \Lambda(\varepsilon k_3 + \theta\gamma) + \theta\varepsilon\pi C^* - \theta\gamma\mu N^*,\ Z = \varepsilon N^*(\tau_1 + \mu) + \eta X, \\ &a' = \varepsilon\eta a_S N^* \theta\varepsilon\pi F_1 + a_V \tau_2 (\varepsilon\eta)^2 \pi\omega - N^* k_3 \eta\varepsilon^2 \omega F_1, \\ &b' = \varepsilon\eta a_S N^*(A_0 F_1 + \theta\varepsilon\pi F_0) + \eta a_V \varepsilon\tau_1 N^* \theta\varepsilon\pi + \eta a_V \tau_2 (G_0\varepsilon\pi + B_0\eta\varepsilon\omega) - \varepsilon N^* k_3 (G_0 F_1 + F_0\eta\varepsilon\omega), \\ &c' = \varepsilon\eta a_S N^* A_0 F_0 + \eta a_V \varepsilon\tau_1 N^* A_0 + \eta a_V \tau_2 G_0 B_0 - \varepsilon N^* k_3 G_0 F_0. \\ &a_S = \frac{1-\phi}{k_2} + \frac{\alpha\phi}{k_1 k_2} + \frac{\omega\phi}{k_1},\ a_V = \frac{\alpha\xi\sigma}{k_1 k_2} + \frac{\xi(1-\sigma)}{k_2} + \frac{\omega\xi\sigma}{k_1},\ G_0 = \varepsilon N^*(\tau_1 + \mu) + \eta\Lambda, \\ &B_0 = \gamma(\Lambda - \mu N^*),\ F_0 = \mu + \frac{\xi\eta\Lambda}{\varepsilon N^*} - \frac{\xi\eta\mu}{\varepsilon},\ F_1 = \frac{\xi\eta\omega}{N^*}, \text{ and } A_0 = \Lambda(\varepsilon k_3 + \theta\gamma) - \theta\gamma\mu N^*. \end{aligned}$$

3.7 | Local Stability of the Endemic Equilibrium Point

To establish the local asymptotic stability of the endemic equilibrium, we evaluate (23) at $E_e = (S^*, C^*, I^*, R^*, V^*)$, which gives

$$\begin{bmatrix} -d_1\lambda_i - (\tau_1 + \mu + \beta^*) & -\eta\omega\frac{S^*}{N^*} & -\eta\frac{S^*}{N^*} & \theta & 0 \\ \phi\beta^* & -d_2\lambda_i + A_{22} - k_1 & A_{23} & 0 & \xi\sigma\beta^* \\ (1-\phi)\beta^* & A_{32} & -d_3\lambda_i + A_{33} - k_2 & 0 & \xi(1-\sigma)\beta^* \\ 0 & \pi & \gamma & -d_4\lambda_i - k_3 & 0 \\ \tau_1 & -\xi\eta\omega\frac{V^*}{N^*} & -\xi\eta\frac{V^*}{N^*} & \tau_2 & -d_5\lambda_i - \mu - \xi\beta^* \end{bmatrix}, \tag{29}$$

where

$$\begin{aligned} \beta^* &= \eta\left(\frac{I^* + \omega C^*}{N^*}\right), \\ A_{22} &= \phi\eta\omega\frac{S^*}{N^*} + \xi\sigma\eta\omega\frac{V^*}{N^*}, \\ A_{23} &= \phi\eta\frac{S^*}{N^*} + \xi\sigma\eta\frac{V^*}{N^*}, \\ A_{32} &= (1-\phi)\eta\omega\frac{S^*}{N^*} + \alpha + \xi(1-\sigma)\eta\omega\frac{V^*}{N^*}, \\ A_{33} &= (1-\phi)\eta\frac{S^*}{N^*} + \xi(1-\sigma)\eta\frac{V^*}{N^*}. \end{aligned}$$

Using the stability test based on Gershgorin circles theorem in [47] (Proposition 3.1), the first hypothesis of Gershgorin circles theorem in [47] (Proposition 3.1) holds provided $A_{22} < d_2\lambda_i + k_1$ and $A_{33} < d_3\lambda_i + k_2$. The second hypothesis is verified if and only if

$$\eta(\omega + 1)\frac{S^*}{N^*} + \theta < d_1\lambda_i + (\tau_1 + \mu + \beta^*), \tag{30}$$

$$\phi\beta^* + A_{23} + \xi\sigma\beta^* < d_2\lambda_i + k_1 + A_{22}, \tag{31}$$

$$(1-\phi)\beta^* + A_{32} + \xi(1-\sigma)\beta^* < d_3\lambda_i + k_2 + A_{33}, \tag{32}$$

$$\pi + \gamma < d_4\lambda_i + k_3, \tag{33}$$

$$\tau_1 + \tau_2 + \xi\eta(\omega + 1)\frac{V^*}{N^*} < d_5\lambda_i + \mu + \xi\beta^*. \tag{34}$$

Thus, the endemic equilibrium E_e is locally asymptotically stable whenever all of the above inequalities hold.

3.8 | Global Stability of the Endemic Equilibrium Point

Theorem 3. *If $\mathcal{R}_e > 1$, the endemic equilibrium E_e of the system (1) is globally asymptotically stable.*

Proof. Consider the candidate Lyapunov function of the form

$$W(t) = \int_\Omega W_1(x,t)dx,$$

where

$$\begin{aligned} W_1(x,t) = &\left(S - S^* + S^*\ln\left(\frac{S^*}{S}\right)\right) + \left(C - C^* + C^*\ln\left(\frac{C^*}{C}\right)\right) \\ &+\left(I - I^* + I^*\ln\left(\frac{I^*}{I}\right)\right) \\ &+\left(R - R^* + R^*\ln\left(\frac{R^*}{R}\right)\right) \\ &+\left(V - V^* + V^*\ln\left(\frac{V^*}{V}\right)\right). \end{aligned}$$

Differentiating $W(t)$ with respect to time t gives

$$\begin{aligned} \frac{dW}{dt} = &\int_\Omega \left[\left(1 - \frac{S^*}{S}\right)\frac{\partial S}{\partial t} + \left(1 - \frac{C^*}{C}\right)\frac{\partial C}{\partial t} + \left(1 - \frac{I^*}{I}\right)\frac{\partial I}{\partial t}\right. \\ &\left.+\left(1 - \frac{R^*}{R}\right)\frac{\partial R}{\partial t} + \left(1 - \frac{V^*}{V}\right)\frac{\partial V}{\partial t}\right]dx. \end{aligned}$$

Substituting for $\frac{\partial S}{\partial t}$, $\frac{\partial C}{\partial t}$, $\frac{\partial I}{\partial t}$, $\frac{\partial R}{\partial t}$, and $\frac{\partial V}{\partial t}$ from model equations in (1) gives

$$\begin{aligned} \frac{dW}{dt} = &\int_\Omega \left(1 - \frac{S^*}{S}\right)d_1\Delta S + \left(1 - \frac{C^*}{C}\right)d_2\Delta C \\ &+\left(1 - \frac{I^*}{I}\right)d_3\Delta I + \left(1 - \frac{R^*}{R}\right)d_4\Delta R \\ &+\left(1 - \frac{V^*}{V}\right)d_5\Delta V\Big]dx + \int_\Omega \left(1 - \frac{S^*}{S}\right) \\ &[\Lambda + \theta R - \tau_1 S - \mu S - \beta S]dx \\ &+\int_\Omega \left(1 - \frac{C^*}{C}\right)[\phi\beta S + \xi\sigma\beta V - (\mu + \alpha + \pi)C]dx \quad (35) \\ &+\int_\Omega \left(1 - \frac{I^*}{I}\right) \\ &[(1-\phi)\beta S + \alpha C + \xi(1-\sigma)\beta V - (\mu + \varepsilon + \gamma)I]dx \\ &+\int_\Omega \left(1 - \frac{R^*}{R}\right)[\pi C + \gamma I - (\mu + \theta + \tau_2)R]dx \\ &+\int_\Omega \left(1 - \frac{V^*}{V}\right)[\tau_1 S + \tau_2 R - \mu V - \xi\beta V]dx. \end{aligned}$$

Applying Green's formula and the Neumann boundary conditions in (3), we obtain

$$\int_\Omega \left(1 - \frac{S^*}{S}\right)d_1\Delta S dx = -d_1\int_\Omega \frac{S^*}{S^2}|\nabla S|^2 dx \le 0,$$

$$\int_\Omega \left(1 - \frac{C^*}{C}\right)d_2\Delta C\, dx = -d_2\int_\Omega \frac{C^*}{C^2}|\nabla C|^2\, dx \le 0,$$

$$\int_\Omega \left(1 - \frac{I^*}{I}\right)d_3\Delta I\, dx = -d_3\int_\Omega \frac{I^*}{I^2}|\nabla I|^2\, dx \le 0,$$

$$\int_\Omega \left(1 - \frac{R^*}{R}\right)d_4\Delta R\, dx = -d_4\int_\Omega \frac{R^*}{R^2}|\nabla R|^2\, dx \le 0,$$

$$\int_\Omega \left(1 - \frac{V^*}{V}\right)d_5\Delta V\, dx = -d_5\int_\Omega \frac{V^*}{V^2}|\nabla V|^2\, dx \le 0.$$

Thus, the expression for $\frac{dW}{dt}$ in (35) simplifies to

$$\begin{aligned} \frac{dW}{dt} \le &\int_\Omega \Big[\Lambda + \theta R - (\tau_1 + \mu + \beta)S - \Lambda\frac{S^*}{S} - \theta R\frac{S^*}{S} + (\tau_1 + \mu + \beta)S^* + \phi\beta S + \xi\sigma\beta V - (\mu + \alpha + \pi)C \\ &- \phi\beta S\frac{C^*}{C} - \xi\sigma\beta V\frac{C^*}{C} + (\mu + \alpha + \pi)C^* + (1-\phi)\beta S + \alpha C + \xi(1-\sigma)\beta V - (\mu + \varepsilon + \gamma)I \\ &- (1-\phi)\beta S\frac{I^*}{I} - \alpha C\frac{I^*}{I} - \xi(1-\sigma)\beta V\frac{I^*}{I} + (\mu + \varepsilon + \gamma)I^* + \pi C + \gamma I - (\mu + \theta + \tau_2)R - \pi C\frac{R^*}{R} \\ &- \gamma I\frac{R^*}{R} + (\mu + \theta + \tau_2)R^* + \tau_1 S + \tau_2 R - \mu V - \xi\beta V - \tau_1 S\frac{V^*}{V} - \tau_2 R\frac{V^*}{V} + \mu V^* + \xi\beta V^*\Big]dx. \end{aligned}$$

Let M denote the collection of positive terms, and N the collection of negative terms so that

$$\frac{dW}{dt} \le M - N,$$

where

$$\begin{aligned} M = &\int_\Omega [\Lambda + \theta R + (\tau_1 + \mu + \beta)S^* + \phi\beta S + \xi\sigma\beta V + (\mu + \alpha + \pi)C^* + (1-\phi)\beta S + \alpha C \\ &+\xi(1-\sigma)\beta V + (\mu + \varepsilon + \gamma)I^* + \pi C + \gamma I + (\mu + \theta + \tau_2)R^* + \tau_1 S + \tau_2 R + \mu V^* + \xi\beta V^*]dx, \end{aligned}$$

$$N = \int_{\Omega} \Big[(\tau_1 + \mu + \beta)S + \Lambda \frac{S^*}{S} + \theta R \frac{S^*}{S} + (\mu + \alpha + \pi)C + \phi\beta S \frac{C^*}{C} + \xi\sigma\beta V \frac{C^*}{C} + (\mu + \varepsilon + \gamma)I + (1-\phi)\beta S \frac{I^*}{I} + \alpha C \frac{I^*}{I} + \xi(1-\sigma)\beta V \frac{I^*}{I} + (\mu + \theta + \tau_2)R + \pi C \frac{R^*}{R} + \gamma I \frac{R^*}{R} + \mu V + \xi\beta V + \tau_1 S \frac{V^*}{V} + \tau_2 R \frac{V^*}{V} \Big] dx.$$

Hence, if $M < N$, then $\frac{dW}{dt} < 0$. Furthermore, $\frac{dW}{dt} = 0$ if and only if $S = S^*$, $C = C^*$, $I = I^*$, $R = R^*$, $V = V^*$ thus the largest compact invariant set in $\{(S, C, I, R, V) \in \Omega, \frac{dW}{dt} = 0\}$ is the singleton set E_e. By Lasalle's invariant principle in [46], for $\mathcal{R}_e > 1$, this implies that E_e is globally asymptotically stable in Ω. □

3.9 | Impact of Parameter Values on the Effective Reproduction Number: A Sensitivity Analysis

A detailed sensitivity analysis of the effective reproduction number, $\mathcal{R}_e$, is performed in order to identify the key parameters governing pneumococcal pneumonia transmission. It quantifies the relative change in $\mathcal{R}_e$ resulting from a relative change in a given parameter, thereby providing critical guidance for targeted intervention strategies. Following the method in [8, 26, 48], the sensitivity index of $\mathcal{R}_e$ with respect to parameter ν is given by

$$\Upsilon_{\nu}^{\mathcal{R}_e} = \frac{\partial \mathcal{R}_e}{\partial \nu} \times \frac{\nu}{\mathcal{R}_e},$$

where ν represents any of the parameters $k, p, \pi, \tau_1, \gamma, \mu, \alpha, \varepsilon, \phi, \omega, \xi, \sigma$.

Consider for instance the transmission contact rate k with

$$\mathcal{R}_e = \frac{kp}{k_1 k_2 (\tau_1 + \mu)} [(\phi\mu + \xi\sigma\tau_1)(k_2\omega + \alpha) + k_1((1-\phi)\mu + \xi(1-\sigma)\tau_1)].$$

The sensitivity index of parameter k is computed as follows

$$\Upsilon_k^{\mathcal{R}_e} = \frac{\partial \mathcal{R}_e}{\partial k} \times \frac{k}{\mathcal{R}_e} = \frac{p}{k_1 k_2 (\tau_1 + \mu)} [(\phi\mu + \xi\sigma\tau_1)(k_2\omega + \alpha) + k_1((1-\phi)\mu + \xi(1-\sigma)\tau_1)] \times \frac{k k_1 k_2 (\tau_1 + \mu)}{kp[(\phi\mu + \xi\sigma\tau_1)(k_2\omega + \alpha) + k_1((1-\phi)\mu + \xi(1-\sigma)\tau_1)]}$$

Thus,

$$\Upsilon_k^{\mathcal{R}_e} = \frac{\partial \mathcal{R}_e}{\partial k} \times \frac{k}{\mathcal{R}_e} = 1.$$

Likewise, the sensitivity indices corresponding to the remaining parameters involved in the effective reproduction number $\mathcal{R}_e$ are evaluated using the same approach. Using the parameter values in Table 1, the corresponding sensitivity indices are generated as presented in Table 2.

3.10 | Sensitivity Analysis Interpretation

From Table 2, it is observed that parameters k, p, ω, ϕ, ξ, and σ, have positive sensitivity indices, meaning that increases in these parameters lead to an increase in $\mathcal{R}_e$, thereby enhancing the persistence of pneumococcal pneumonia. In contrast, parameters such as τ_1, π, γ, α, and ε exhibit negative sensitivity indices, implying that their increase contributes to reducing $\mathcal{R}_e$ and thus suppresses disease persistence. By prioritizing the reduction of parameters that drive an increase in $\mathcal{R}_e$ and reinforcing those that reduce it, policymakers and healthcare practitioners can formulate effective interventions aimed at lowering pneumococcal pneumonia spread and improving public health outcomes.

To easily visualize how each parameter affects disease transmission, each subplot in Figure 2 shows a one at a time variation of a single parameter while keeping the others constant.

4 | Numerical Simulations

This section presents numerical simulations of the model system (1). MATLAB was used to perform the simulations, employing finite difference methods to numerically solve the system and investigate the combined effects of spatial–temporal variations, vaccination, and treatment on the transmission dynamics of pneumococcal pneumonia. The parameter values used were mainly from literature (Table 1), where necessary assumptions were made in order to have more realistic simulation results. The following initial conditions were considered; $S_0 = 400 + 8\cos(x)$, $C_0 = 150 + \cos(x)$, $I_0 = 200 + \cos(x)$, $R_0 = 140 + \cos(x)$, and $V_0 = 150 + \cos(x)$ so as to have a wave like propagation of the disease, with diffusion coefficients in units of $m^2 day^{-1}$: $d_1 = 0.1$, $d_2 = 0.05$, $d_3 = 0.02$, $d_4 = 0.1$, $d_5 = 0.3$.

TABLE 2 | Numerical values of sensitivity indices of $\mathcal{R}_e$.

Parameter symbols	Sensitivity indices
k	+1.0000
p	+1.0000
ω	+0.4811
ϕ	+0.3811
ξ	+0.0625
σ	+0.0180
τ_1	−0.9131
ε	−0.4646
π	−0.2415
α	−0.2332
γ	−0.0534

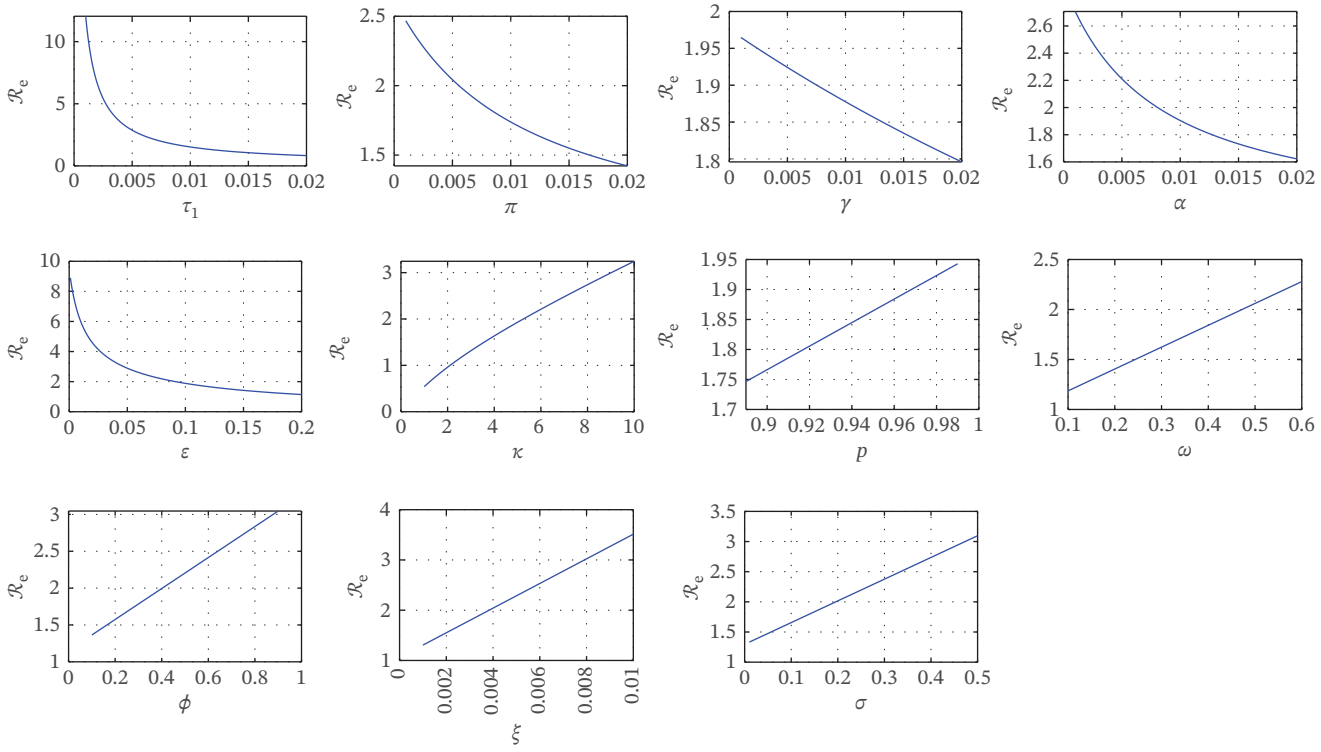


FIGURE 2 | Visualization of how various model parameters influence the effective reproduction number $\mathscr{R}_e$.

4.1 | Spatial-Temporal Dynamics of Pneumococcal Pneumonia When $\mathscr{R}_e<1$

Figure 3 shows the spatial–temporal evolution of pneumococcal pneumonia, obtained using the parameter values provided in Table 1, for which the effective reproduction number is $\mathscr{R}_e = 0.3493<1$. In this case, it is observed that the solution (S, C, I, R, V) of system (1) converges to the disease-free equilibrium E_0 as $t \to \infty$. This implies that the disease-free equilibrium E_0 is globally asymptotically stable, and the infection cannot persist in the population when the effective reproduction number remains below unity, $\mathscr{R}_e<1$. This is consistent with the theoretical findings in Theorem 2 confirming that the disease eventually dies out when $\mathscr{R}_e<1$.

4.2 | Spatial-Temporal Dynamics of Pneumococcal Pneumonia When $\mathscr{R}_e>1$

Figure 4 shows the spatial–temporal evolution of pneumococcal pneumonia, obtained using the parameter values provided in Table 1, but with $\tau_1 = 0.0001$, $\tau_2 = 0.0003$, and $p = 0.1$. Under these parameter settings, the effective reproduction number is $\mathscr{R}_e = 5.0329>1$. In this case, it is observed that the solution of system (1) converges to the endemic equilibrium E_e as $t \to \infty$. This observed convergence confirms the global asymptotic stability of the endemic equilibrium E_e, aligning with theoretical findings in Theorem 3.

4.2.1 | Intervention Strategies

Here, the temporal dynamics of disease progression under different intervention strategies, namely vaccination and treatment, are investigated. The graphical results are generated using the ODE form of system (1), with initial conditions $S(0) = 1000$, $C(0) = 20$, $I(0) = 10$, $R(0) = 12$, $V(0) = 12$, together with the baseline parameter values provided in Table 1.

4.3 | Effect of Enhanced Treatment on Pneumococcal Pneumonia Dynamics

Figures 5 and 6 illustrate the influence of the treatment rates of carriers and infected individuals, respectively, on the transmission dynamics of pneumococcal pneumonia. The results show that enhancing the treatment rate of carriers significantly reduces both carrier and infected populations, while increasing the treatment rate of infected individuals likewise leads to a marked decline in disease prevalence. In both cases, higher treatment rates accelerate the reduction of infection levels and improve overall disease control. These findings underscore the importance of effective treatment strategies targeting both carriers and infected individuals in reducing pneumococcal pneumonia transmission and sustaining long-term control.

4.4 | Effect of Enhanced Vaccination Rates on Pneumococcal Pneumonia Dynamics

Figure 7 shows the effect of increasing the vaccination rate of susceptible individuals (τ_1) on pneumococcal pneumonia dynamics. As τ_1 increases from 0.01 to 0.04, both carrier and infected populations decline over time and eventually approach zero. This implies that higher vaccination coverage among susceptible individuals can lead to the elimination of pneumococcal pneumonia in the population.

4.5 | Influence of Vaccination and Treatment on Pneumococcal Pneumonia Dynamics

Figure 8 shows the dynamics of carrier and infected populations under treatment alone ($\mathscr{R}_0$) and under the combined strategy of treatment and vaccination ($\mathscr{R}_e$). The results show that integrating vaccination with treatment has a greater influence on the

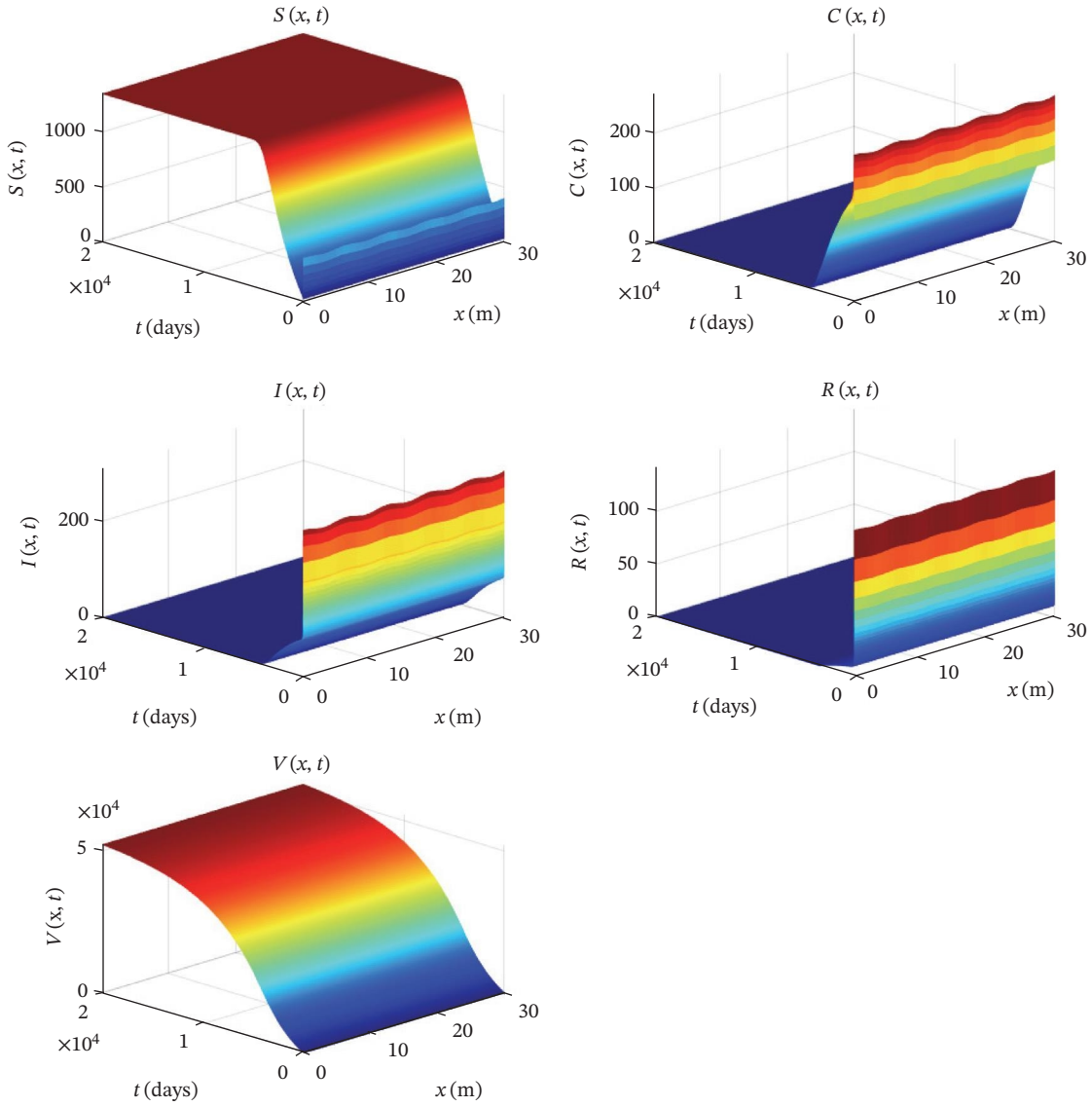


FIGURE 3 | Global asymptotic stability of the disease-free equilibrium E_0.

reduction of pneumococcal pneumonia compared to relying on treatment alone.

4.6 | Impact of Vaccine Nonresponsiveness on the Transmission Dynamics of Pneumococcal Pneumonia

Figure 9 shows the impact of vaccine failure rate, ξ on carriers and infected individuals. Low ξ, reflecting effective vaccination, both carrier and infected classes decrease progressively and approach elimination, while high ξ leads to an increase in both carriers and infected individuals, indicating persistent transmission and higher endemic levels. These results show the impact of vaccine failure on disease prevalence, with decreased vaccine failure leading to better control of pneumococcal pneumonia.

5 | Discussion and Conclusion

In this study, an SCIRV reaction-diffusion model for pneumococcal pneumonia incorporating vaccination and treatment was formulated and analyzed. The model was shown to be well-posed and biologically relevant. The analysis revealed that the model admitted two equilibrium points, that is, the disease-free equilibrium and the endemic equilibrium. The effective reproduction number, $\mathcal{R}_e$, was then derived as the threshold parameter governing disease dynamics. The disease-free equilibrium E_0 was found to be locally and globally asymptotically stable whenever $\mathcal{R}_e < 1$. The conditions for the endemic equilibrium E_e being locally asymptotically stable were established using the Gershgorin Circle Theorem and also it was found that the endemic equilibrium E_e was globally asymptotically stable whenever $\mathcal{R}_e > 1$.

Sensitivity analysis identified the contact rate (k), transmission probability (p), vaccine failure rate (ξ), and related parameters (ω, ϕ, σ) positively influenced disease transmission by increasing $\mathcal{R}_e$, while parameters such as the vaccination rate of susceptibles τ_1, the recovery rates due to treatment of carriers π and infected γ, exhibit negative sensitivity indices, indicating that their increase reduced $\mathcal{R}_e$ and thus suppressing disease persistence. Numerical simulations confirmed that the disease is eliminated when $\mathcal{R}_e < 1$

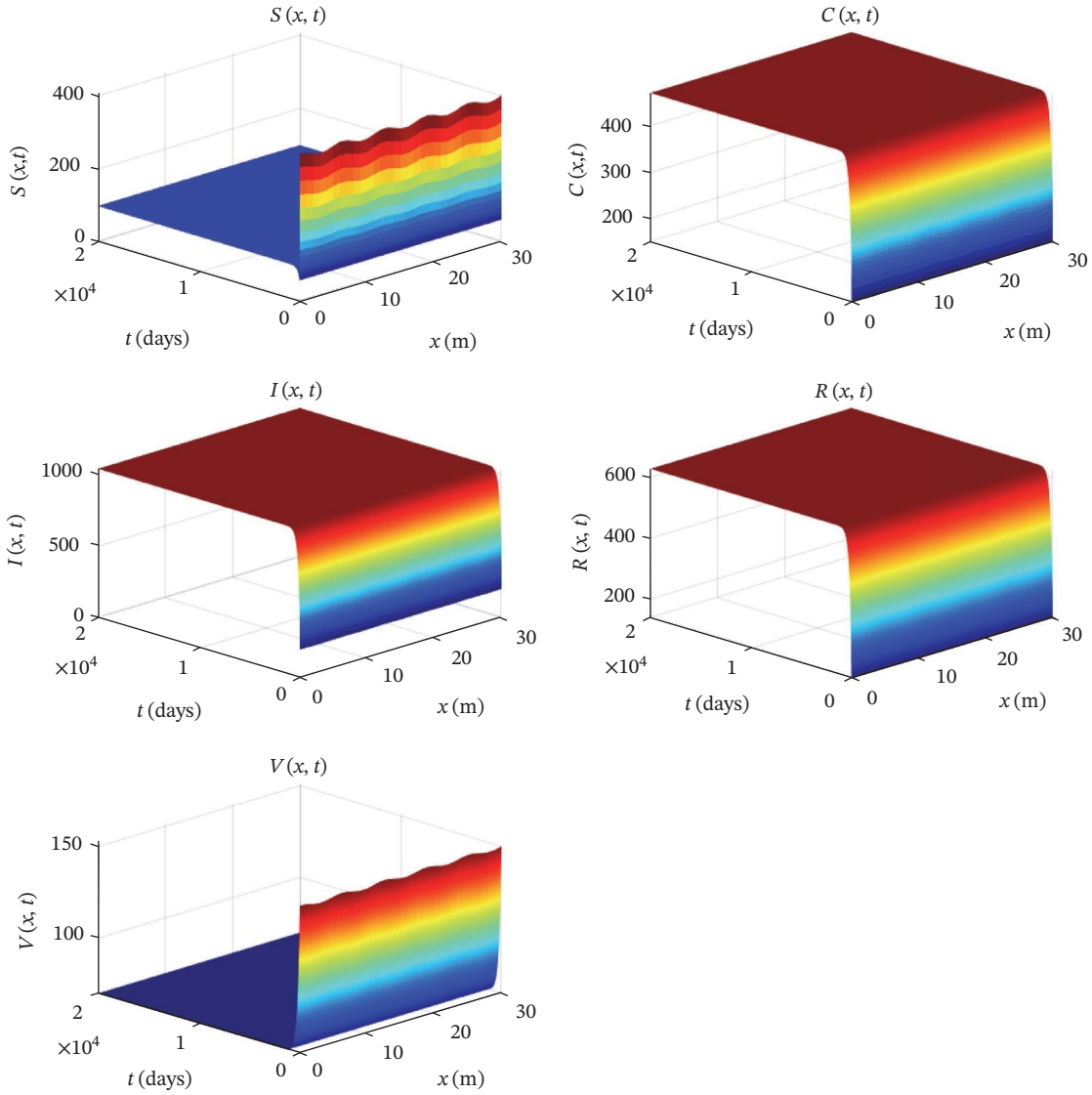


FIGURE 4 | Global asymptotic stability of the endemic equilibrium E_e.

and persists when $\mathscr{R}_e > 1$. The results further demonstrate that increasing treatment rates substantially reduces disease prevalence, while increasing vaccination among susceptible individuals has the strongest impact on eliminating the disease. A combined strategy of vaccination and treatment was shown to be more effective than treatment alone, whereas elevated vaccine failure rates were observed to weaken overall control efforts.

Based on these results, we recommend that governments and health ministries prioritize early massive vaccination campaigns in high-risk areas and implement a combined strategy of vaccination and treatment. Additionally, screening and diagnostic testing should be implemented, with positive cases subjected to timely medical treatment. Future work could extend this model to incorporate other strategies, such as improved nutrition, exclusive breastfeeding, enhanced surveillance for antibiotic-resistant strains, and timely diagnosis. This model could also be extended to a stochastic framework to better capture the uncertainty in disease dynamics.

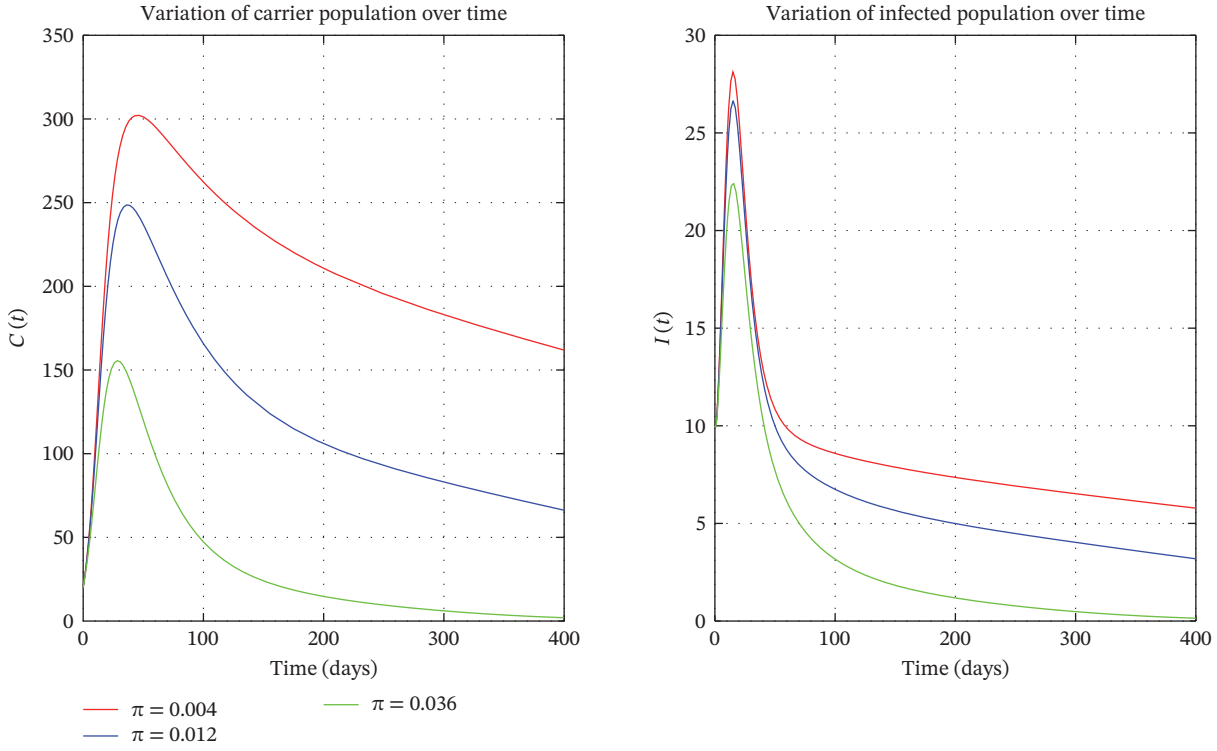


FIGURE 5 | Effect of carrier treatment rate on the transmission dynamics of pneumococcal pneumonia.

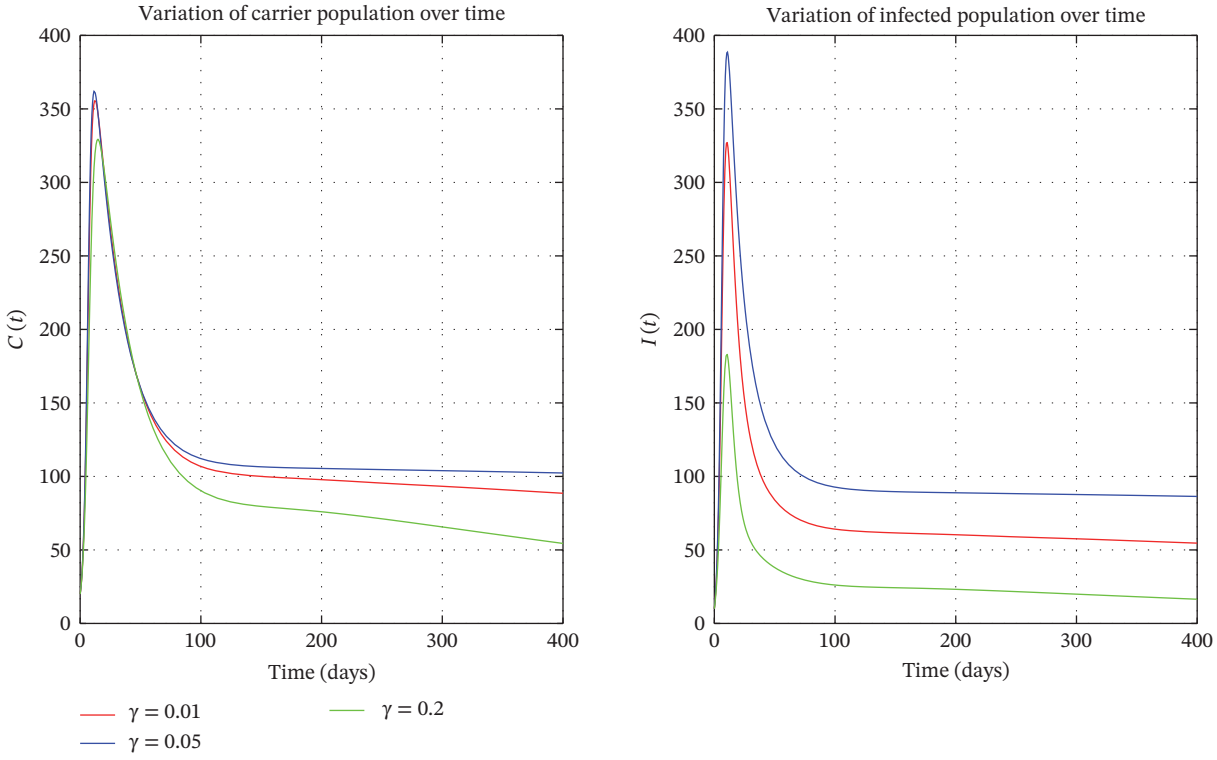


FIGURE 6 | Influence of infected-individual treatment rates on pneumococcal pneumonia transmission dynamics.

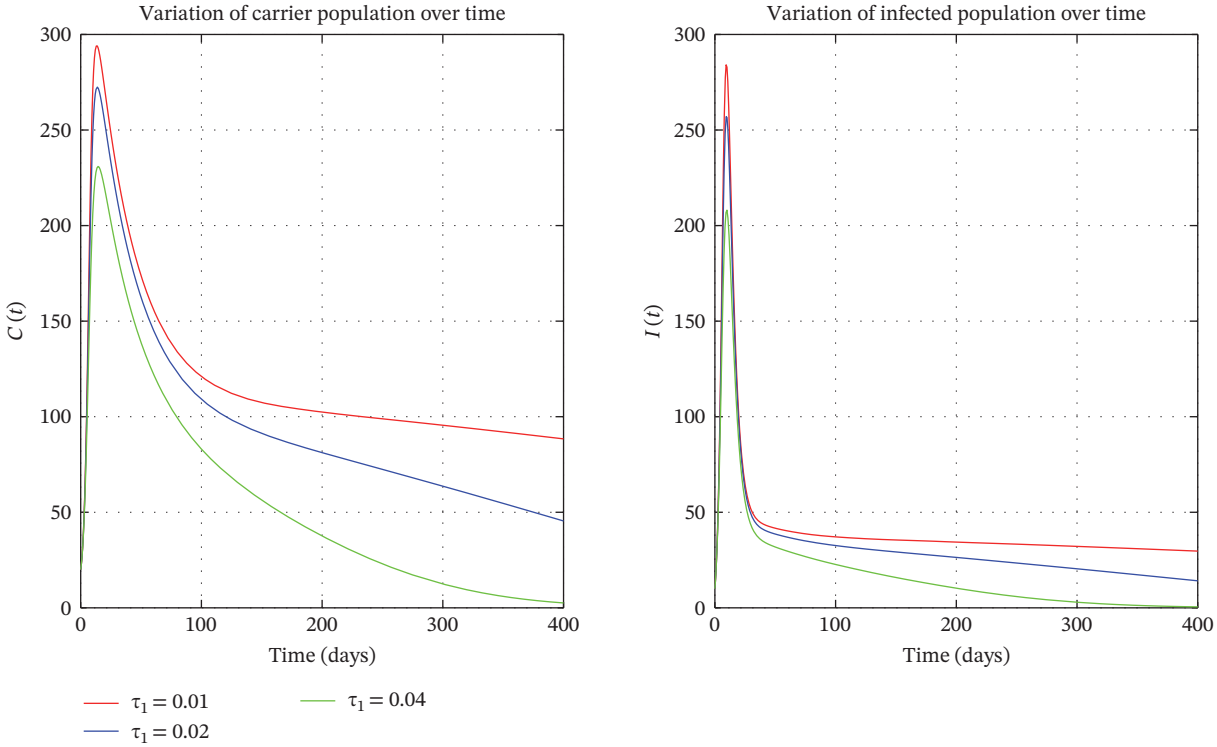


FIGURE 7 | Impact of varying the vaccination rate of susceptible individuals on the transmission dynamics of pneumococcal pneumonia.

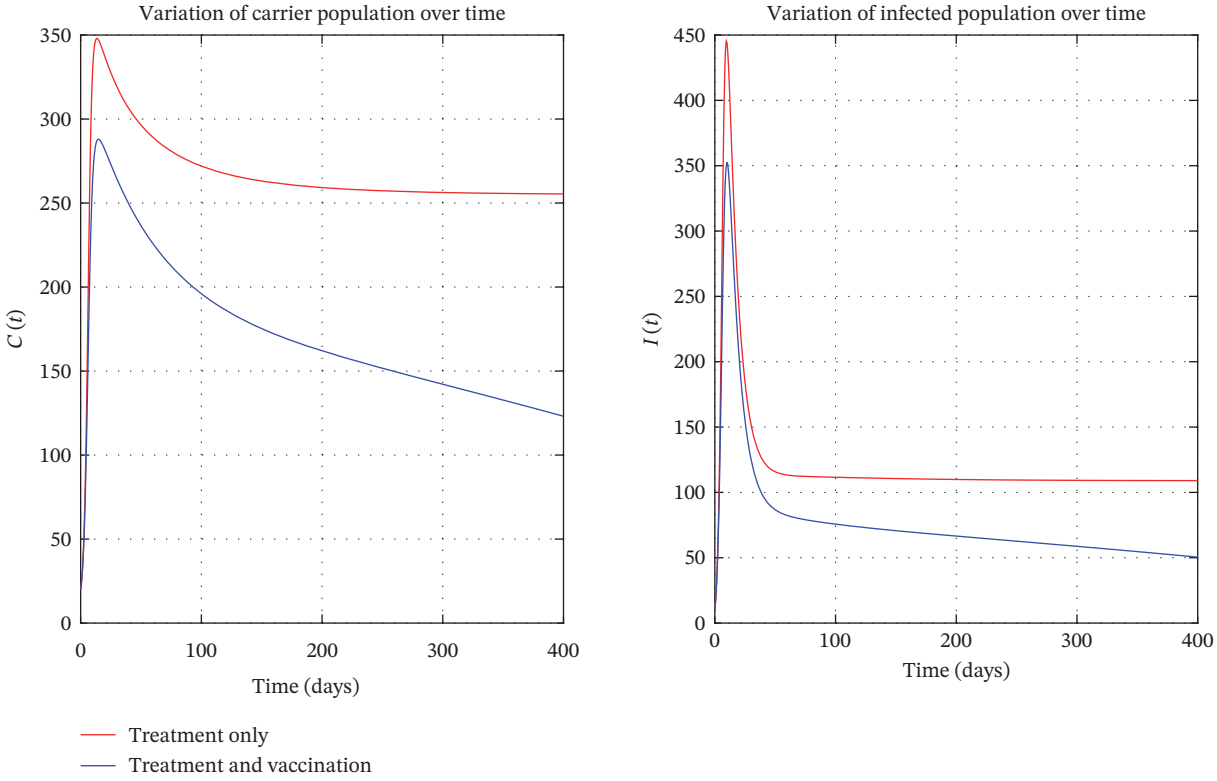


FIGURE 8 | Influence of vaccination and treatment on pneumococcal pneumonia dynamics.

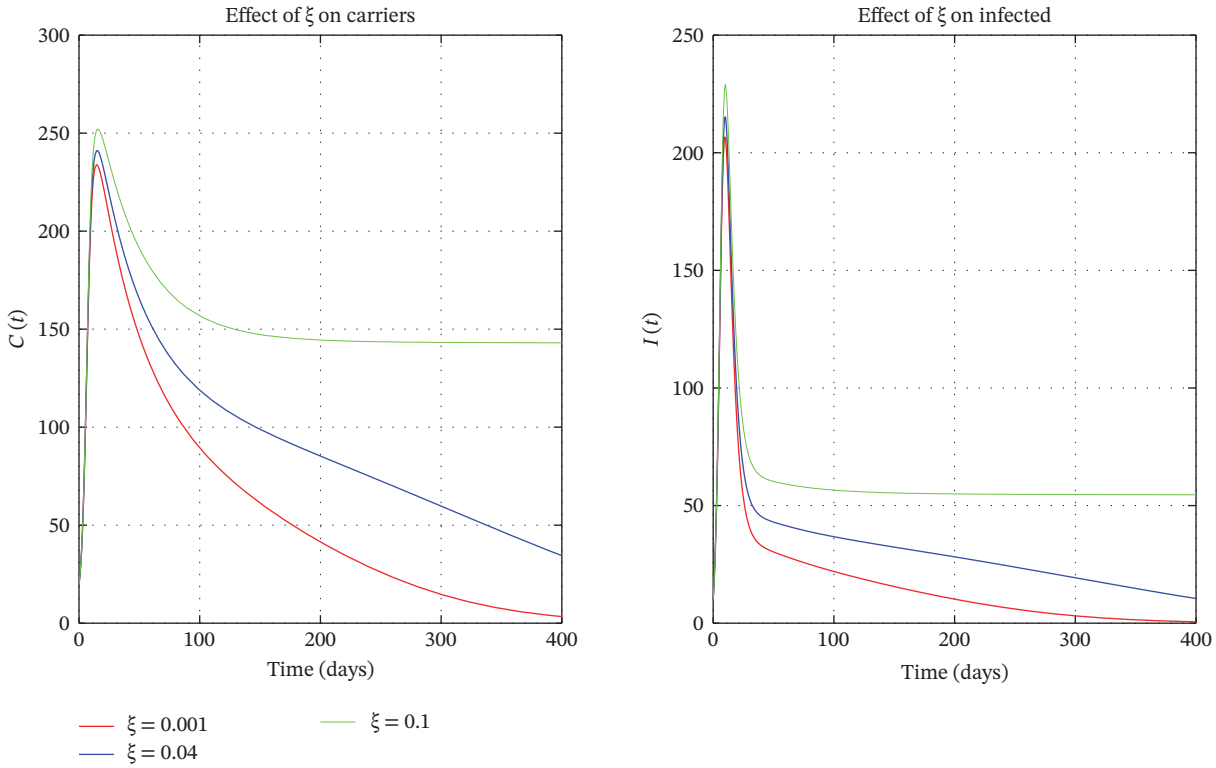


FIGURE 9 | Impact of vaccine failure on the dynamics of carriers and infected individuals.

Funding

No funding was received for this study.

Conflicts of Interest

The authors declare no conflicts of interest.

Data Availability Statement

Data sharing is not applicable to this article as no datasets were generated or analyzed during the current study.

References

1. J. Alya, D. Aldila, and R. Rusin, "A Mathematical Model of the Spread of Pneumococcal Pneumonia Disease by Considering Vaccine and Hospital Care Interventions," in *AIP Conference Proceedings*, 2498, (AIP Publishing, 2022).

2. World Health Organization, "Fact Sheet on Pneumonia," *Weekly Epidemiological Record* 88, no. 11 (2013): 126-127.

3. M. Byamukama, D. Kajunguri, and M. Karuhanga, "Optimal Control Analysis of Pneumonia and HIV/AIDS Co-Infection Model," *Mathematics Open* 03 (2024): 2450006.

4. D. A. Watson, D. M. Musher, J. W. Jacobson, and J. Verhoef, "A Brief History of the Pneumococcus in Biomedical Research: A Panoply of Scientific Discovery," *Clinical Infectious Diseases* 17, no. 5 (1993): 913–924.

5. P. Pahal, V. Rajasurya, and A. D. Nguyen, "Typical Bacterial Pneumonia," (StatPearls, 2018).

6. World Health Organization, *Global Health Estimates 2016: Deaths by Cause, Age, Sex, by Country and by Region, 2000–2016* (World Health Organization, 2018): 1242–1247.

7. F. K. Mbabazi, J. Mugisha, and M. Kimathi, "Global Stability of Pneumococcal Pneumonia With Awareness and Saturated Treatment," *Journal of Applied Mathematics* 2020, no. 1 (2020): 3243957.

8. M. Kizito and J. Tumwiine, "A Mathematical Model of Treatment and Vaccination Interventions of Pneumococcal Pneumonia Infection Dynamics," *Journal of Applied Mathematics* 2018, no. 1 (2018): 2539465.

9. D. Aldila, N. Awdinda, Fatmawati, F. F. Herdicho, M. Z. Ndii, and C. W. Chukwu, "Optimal Control of Pneumonia Transmission Model With Seasonal Factor: Learning From Jakarta Incidence Data," *Heliyon* 9, no. 7 (2023): e18096.

10. R. H. Chisholm, P. T. Campbell, Y. Wu, S. Y. Tong, J. McVernon, and N. Geard, "Implications of Asymptomatic Carriers for Infectious Disease Transmission and Control," *Royal Society Open Science* 5, no. 2 (2018): 172341.

11. F. K. Mbabazi, J. Y. Mugisha, and M. Kimathi, "Hopf-Bifurcation Analysis of Pneumococcal Pneumonia With Time Delays," *Abstract and Applied Analysis* 2019 (2019): 3757036.

12. A. Torres, F. Blasi, N. Dartois, and M. Akova, "Which Individuals Are at Increased Risk of Pneumococcal Disease and Why? Impact of Copd, Asthma, Smoking, Diabetes, and/or Chronic Heart Disease on Community-Acquired Pneumonia and Invasive Pneumococcal Disease," *Thorax* 70, no. 10 (2015): 984–989.

13. B. Farr, C. Bartlett, J. Wadsworth, and D. Miller, "Risk Factors for Community-Acquired Pneumonia Diagnosed Upon Hospital Admission," *Respiratory Medicine* 94, no. 10 (2000): 954–963.

14. S. Qazi, S. Aboubaker, R. MacLean, et al., "Ending Preventable Child Deaths From Pneumonia and Diarrhoea by 2025. development of the Integrated Global Action Plan for the Prevention and Control of Pneumonia and Diarrhoea," *Archives of Disease in Childhood* 100, no. Suppl 1 (2015): S23–S28.

15. M. J. Tobin, "Diagnosis of Pneumonia: Techniques and Problems," *Clinics in Chest Medicine* 8, no. 3 (1987): 513–527.

16. G. B. Grant, H. Campbell, S. F. Dowell, et al., "Recommendations for Treatment of Childhood Non-Severe Pneumonia," *The Lancet Infectious Diseases* 9, no. 3 (2009): 185–196.

17. A. Gentile and V. Bazán, "Prevention of Pneumococcal Disease Through Vaccination," *Vaccine* 29 (2011): C15–C25.

18. K. Yatera and K. Yamasaki, "Management of the Diagnosis and Treatment of Pneumonia in an Aging Society," *Internal Medicine* 64, no. 4 (2025): 503–517.

19. F. Russell and E. K. Mulholland, "Recent Advances in Pneumococcal Vaccination of Children," *Annals of Tropical Paediatrics* 24, no. 4 (2013): 283–294.

20. S. Moberley, J. Holden, D. P. Tatham, and R. M. Andrews, "Vaccines for Preventing Pneumococcal Infection in Adults," *Cochrane Database of Systematic Reviews* 2013, no. 1 (2013).

21. M. Byamukama and M. Kizito, "Optimizing Protection and Treatment Strategies for Childhood Pneumonia amid Vaccine-Unresponsive Serotypes," *Journal of Applied Mathematics and Physics* 13, no. 5 (2025): 1834–1857.

22. J. S. Ngocho, B. Magoma, G. A. Olomi, et al., "Effectiveness of Pneumococcal Conjugate Vaccines Against Invasive Pneumococcal Disease Among Children Under 5 Years of Age in Africa: A Systematic Review," *PLoS ONE* 14, no. 2 (2019): e0212295.

23. S. Bentout and S. Djilali, "Asymptotic Dynamics of SIRS Epidemic Model With Dispersal Budgets and Nonlinear Rates About Heterogenous Environments," *Mathematical Modelling of Natural Phenomena* 20 (2025): 17.

24. B. Soufiane and T. M. Touaoula, "Global Analysis of an Infection Age Model With a Class of Nonlinear Incidence Rates," *Journal of Mathematical Analysis and Applications* 434, no. 2 (2016): 1211–1239.

25. D. J. Temfack Nguefack, "Mathematical Modeling of Schistosomiasis Transmission Using Reaction-Diffusion Equations," *Fundamental Journal of Mathematics and Applications* 7, no. 2 (2024): 118–136.

26. B. Kammegne, K. Oshinubi, O. Babasola, et al., "Mathematical Modelling of the Spatial Distribution of a COVID-19 Outbreak With Vaccination Using Diffusion Equation," *Pathogens* 12, no. 1 (2023): 88.

27. S. Bentout, S. Djilali, and P. A. Naik, "Asymptotic Profiles of a Generalized Reaction-Diffusion Viral-Infection Model With Logistic Source," *Journal of Mathematical Analysis and Applications* (2025): 130146.

28. S. Bentout, "Dynamics of a Nonlocal Diffusion Virus Model With Age Structure, Heterogeneity, Nonlinear Incidence Rates and Time Delays," *International Journal of Modelling and Simulation* (2025): 1–27.

29. S. Bentout, "Analysis of Global Behavior in an Age-Structured Epidemic Model With Nonlocal Dispersal and Distributed Delay," *Mathematical Methods in the Applied Sciences* 47, no. 9 (2024): 7219–7242.

30. B. Guenad, S. Djilali, and S. Bentout, "Behavior of a Nonlocal Species-Pathogen System With Varied Dispersal Mechanisms in Heterogeneous Habitats," *Journal of Computational and Applied Mathematics* 482 (2026): 117341.

31. S. Bentout, "Analysis of Traveling Wave Solutions for an SIS Model With Age Structure," *Zeitschrift für Angewandte Mathematik und Physik* 77, no. 2 (2026): 79.

32. V. Davydovych, V. Dutka, and R. Cherniha, "Reaction–Diffusion Equations in Mathematical Models Arising in Epidemiology," *Symmetry* 15, no. 11 (2023): 2025.

33. P. Colli, G. Gilardi, G. Marinoschi, and E. Rocca, "Optimal Control of a Reaction-Diffusion Model Related to the Spread of Covid-19," *Analysis and Applications* 22, no. 1 (2024): 111–136.

34. F. Mahroug and S. Bentout, "Dynamics of a Diffusion Dispersal Viral Epidemic Model With Age Infection in a Spatially Heterogeneous Environment With General Nonlinear Function," *Mathematical Methods in the Applied Sciences* 46, no. 14 (2023): 14983–15010.

35. C. G. Ngari, "Modelling Vaccination and Treatment of Childhood Pneumonia and Their Implications," *Journal of Advances in Mathematics and Computer Science* 28, no. 1 (2018): 1–24.

36. G. T. Tilahun, O. D. Makinde, and D. Malonza, "Modelling and Optimal Control of Pneumonia Disease With Cost-Effective Strategies," *Journal of Biological Dynamics* 11, no. sup2 (2017): 400–426.

37. J. O. Ong'ala, J. Mugisha, and O. Paul, "Mathematical Model for Pneumonia Dynamics With Carriers," *International Journal of Mathematical Analysis* 7, no. 50 (2013): 2457–2473.

38. M. Byamukama, M. Karuhanga, and D. Kajunguri, "Mathematical Analysis of the Role of Treatment and Vaccination in the Management of the HIV/AIDS and Pneumococcal Pneumonia Co-Infection," *Journal of Mathematics* 2025, no. 1 (2025): 5879698.

39. D. Otoo, P. Opoku, S. Charles, and A. P. Kingsley, "Deterministic Epidemic Model for (svcsycasyir) Pneumonia Dynamics, With Vaccination and Temporal Immunity," *Infectious Disease Modelling* 5 (2020): 42–60.

40. J. M. Haugh, "Analysis of Reaction-Diffusion Systems With Anomalous Subdiffusion," *Biophysical Journal* 97, no. 2 (2009): 435–442.

41. S. Bertone, A. Cellina, and E. M. Marchini, "On Hopf's Lemma and the Strong Maximum Principle," *Communications in Partial Differential Equations* 31, no. 5 (2007): 701–733.

42. P. Van den Driessche and J. Watmough, "Further Notes on the Basic Reproduction Number," in *Mathematical Epidemiology*, (Springer, 2008): 159–178.

43. K. E. Lamb, D. Greenhalgh, and C. Robertson, "A Simple Mathematical Model for Genetic Effects in Pneumococcal Carriage and Transmission," *Journal of Computational and Applied Mathematics* 235, no. 7 (2011): 1812–1818.

44. S. Bentout, A. Chekroun, and T. Kuniya, "Parameter Estimation and Prediction for Coronavirus Disease Outbreak 2019 (COVID-19) in algeria," *AIMS Public Health* 7, no. 2 (2020): 306–318.

45. O. Diekmann, J. A. P. Heesterbeek, and J. A. J. Metz, "On the Definition and the Computation of the Basic Reproduction Ratio r 0 in Models for Infectious Diseases in Heterogeneous Populations," *Journal of Mathematical Biology* 28, no. 4 (1990): 365–382.

46. N. Cangiotti, M. Capolli, M. Sensi, and S. Sottile, "A Survey on Lyapunov Functions for Epidemic Compartmental Models," *Bollettino dell'Unione Matematica Italiana* 17, no. 2 (2024): 241–257.

47. D. Bejarano, E. Ibargüen-Mondragón, and E. A. Gómez-Hernández, "A Stability Test for Non Linear Systems of Ordinary Differential Equations Based on the Gershgorin Circles," *Contemporary Engineering Sciences* 11, no. 91 (2018): 4541–4548.

48. N. Chitnis, J. M. Hyman, and J. M. Cushing, "Determining Important Parameters in the Spread of Malaria Through the Sensitivity Analysis of a Mathematical Model," *Bulletin of Mathematical Biology* 70, no. 5 (2008): 1272–1296.

Reproduced with permission of copyright owner. Further reproduction prohibited without permission.